INVOLVEMENT OF MIXED LINEAGE LEUKEMIA AND HOMEOBOX PROTEINS IN DNA DAMAGE RECOGNITION AND REPAIR

by

SOMDUTTA CHAKRABORTY

Presented to the Faculty of the Graduate School of

The University of Texas at Arlington in Partial Fulfillment

of the Requirements

for the Degree of

MASTER OF SCIENCE in BIOENGINEERING

THE UNIVERSITY OF TEXAS AT ARLINGTON

FALL 2012

This is for you, Maa

Acknowledgements

The fact that The United States of America is a land full of opportunities became evident to me a year and a half ago, when I got the chance to work in a research lab on a project that had the potential to make a huge impact in its field of research. I could not be more grateful to my mentor, my advisor Dr. Samarendra Mohanty, for having given me this opportunity. Working with him on my thesis, was my very first exposure to hands on experience regarding the ethics of lab work. Dr. Mohanty has given me the much needed exposure and motivation to continue in the field of research. He has been very critical at times, which in hindsight was necessary. I would like to thank my committee members Dr. Hanli Liu and Dr. Bahong Yuan for taking the time to be a part of my thesis and providing valuable inputs.

I am greatly indebted to Dr. Ling Gu who has guided me and helped me in a huge way. She has taken me step by step, teaching me the basics, which have contributed greatly to my skill set. I extend my gratitude to my colleagues of the Biophysics & Physiology Lab who have been very patient with me and have supported me in their own way. My research work would have been incomplete if not for the support of Dr. Subhrangshu S Mandal and his students, Sahba and Arun who have been a huge help in the Chemistry aspect of my work.

My friends at UTA, who are a family away from home, thanks for the support and the sometime needed emotional boost. Amruta, Ankita, Bipin, Jayanth, Kiran, Nilanjana, Rahul, Sujoy and Sukalpa you all have been an incredible set of friends who have stood by me during this incredible experience. Thank you Bony, you have inspired me and motivated me, in your weird own way, when I much needed it. You have made me smile and cared for me in times when I was a nervous wreck! My ‘Overseas Support System’, a set of friends whom I have known for the last 20 years of my life, Manali, Ruchita, Pooja,

Sharvari and Pritha, I am just glad you all have stuck with me through thick and thin and believed in me more than I did.

Maa and Baba, firstly thank you for providing me with this incredible opportunity. You have inspired me to be as humble and balanced as you two. You have been extremely patient with me and taught me to be passionate about what I do. You taught me it is alright to fail as long as you are willing to get back up and fix it. Thank you for reinstating the faith in myself in times when I found it difficult to. I can never be thankful enough. My grandmother for loving me always and it is a very comforting fact that to her I have been nothing but the best.

Last but not in the least, I am grateful to God and those loved few who are constantly blessing me from high above.

November 15, 2012.

Abstract

INVOLVEMENT OF MIXED LINEAGE LEUKEMIA AND HOMEOBOX PROTEINS IN DNA DAMAGE RECOGNITION AND REPAIR

Somdutta Chakraborty, M.S

The University of Texas at Arlington, 2012

Supervising Professor: Samarendra Mohanty

Deoxyribonucleic Acid (DNA) molecules are informational molecules, encoding genetic information which is indispensable in the development and functioning of living organisms. DNA encodes for most proteins essential for all bodily functions and a few of which are known to be involved in the DNA Damage Response/ Repair mechanism. DNA damage recognition and repair is crucial and the cell has an innate mechanism of repairing it. Unrepaired DNA damage leads to genetic mutation or even cancers, which are sustained by further cell division and genetic multiplication. Other researchers have already confirmed the involvement of several proteins and histones like PARP and H2AX respectively in the DNA damage repair pathway. In this thesis, different proteins like Mixed Lineage Leukemia (MLL) and Homeobox protein Hox-B9 were screened to verify their role in DNA Damage Recognition/ Repair pathway. The response of these proteins upon Laser-induced DNA Damage was analyzed by corresponding anti-body staining as well as by fluorescence time-lapse imaging of GFP (Green Fluorescent Protein) tagged cells. The main aim is to evaluate role of MLLs and HOX proteins in the complex DNA Damage Repair pathway and its associated proteins.

Table of Contents

Acknowledgements iv

Abstract vi

List of Tables xii

Chapter 1 Introduction 1

1.1 Cause of DNA Damage 1

1.2 DNA Damage Repair Pathways 2

1.3 Related Work 4

1.4 Motivation 6

Chapter 2 Materials & Methods 8

2.1 Multimodal Setup 8

2.2 Various Cell Lines 10

2.2.1 HeLa Cells 10

2.2.2 HEK 293 Cells: 11

2.2.3 HT1080 Cells 12

2.3 Cell culture 13

2.4 Marking Region of Interest (ROI) on the dish 14

2.5 Induction of localized DNA damage with the use of laser 14

2.6 Immunostaining 17

2.7 Imaging of Immunostained Cells 19

2.8 Induction of DNA damage by ultrafast laser microbeam and live imaging 19

2.9 Software: ImageJ 20

Chapter 3 Fixed Method 21

3.1 Poly ADP Ribose Polymerase (PARP) 22

3.2 Mixed Lineage Leukemia (MLL) 23
3.3 Results 26
3.3.1 Experiment Set 1 26
3.3.2 Experiment Set 2 27
3.3.3 Experiment Set 3 29
3.3.4 Experiment Set 4 31
3.3.5 Experiment Set 5 32
3.3.6 Experiment Set 6 34
3.3.7 Irradiation Power constant, t^{fix} varied: 35
3.3.7.1 Experiment Set: 7, 8, 9 36
3.3.8 Experiment Set 10 : MLL3 37
3.3.9 Experiment Set 11, 12: MLL-4 38
3.4 Discussion 39
Chapter 4 Live Cell Method 41
4.1 TRF2-YFP 41
4.1.1 Results 41
4.1.1.1 Case 1: Immunostaining 41
4.1.1.2 Case 2: Time-lapse epifluorescence of TRF2 accumulation 42
4.1.2 Discussion 45
4.2 HOXB9- GFP (Over-expressed) 45
4.2.1 Results 46
4.2.1.1 Trail 1 47
4.2.1.2 Trial 2 49
4.2.2 Discussion 50
Chapter 5 Conclusion & Future Work 51

Appendix A List of Abbreviations 54

Appendix B Presentation in Conferences 56

References 58

Biographical Information 64

List of Illustrations

Figure 1-1 Different DNA Damage Repair Pathways 3
Figure 1-2 Possible Mechanisms of DNA Damage [8] 4
Figure 1-3 Wavelength Dependence of DNA Damage [7] 5
Figure 2-1 Multimodal Setup. 8
Figure 2-2 Schematic of the actual Multimodal Setup 10
Figure 2-3 HeLa Cells 11
Figure 2-4 HEK 293 Cells. (L) Bright Field Image (R) Fluorescent Image 12
Figure 2-5 HT1080 cells with TRF2 antibody staining 13
Figure 2-6 Marking the ROI. 14
Figure 2-7 Mai Tai Controller GUI 16
Figure 2-8 Laser beam Profile (L) Unfocused Beam (R) Focused Beam spot. 16
Figure 2-9 PM Micromanager GUI. 17
Figure 3-1 Experimental Flow-chart 21
Figure 3-2 PARP Response Pathway 23
Figure 3-3 Structure of MLL and associated protein sub-units 24
Figure 3-4 Results for MLL-1 (Green) and PARP (Red) 27
Figure 3-5 Results for MLL-1(Green) & Ash-2(Red). 28
Figure 3-6 Results for MLL-1 (Green) and CGBP (Red). 30
Figure 3-7 Results for MLL-1 (Green) & CTD (Red) 32
Figure 3-8 Results for CytC (Green) & MLL-1(Red) 33
Figure 3-9 Results for MLL-1 (Green) & RBBP (Red) 35
Figure 3-10 Results for MLL-1 with varied fixing times 36
Figure 3-11 Results for MLL-3 [15]. 38
Figure 3-12 Results for MLL-4. 39

Figure 4-1 Immunostaining of TRF2 along with TUNEL Assay and γ-H2AX. 42
Figure 4-2 Time-lapse imaging of TRF2 accumulation. 42
Figure 4-3 Kinetics of increase in fluorescence of TRF2-YFP subsequent to fs laser-induced DNA damage Curve fitting to calculate accumulation time for 0.5nJ pulse 43
Figure 4-4 Kinetics of increase in fluorescence of TRF2-YFP subsequent to fs laser-induced DNA damage. Curve fitting to calculate accumulation time for 0.8nJ pulse. 43
Figure 4-5 Graph of TRF2 Accumulation time v/s Pulse Energy. 44
Figure 4-6 TRF2 accumulation time v/s Number of pulses of varying energy. 45
Figure 4-7 HoxB9-GFP (Trail 1). 47
Figure 4-8 Intensity v/s Time plot. 48
Figure 4-9 Normalized Plot. 48
Figure 4-10 HoxB9-GFP (Trial 2). 49
Figure 4-11 Intensity v/s Time plot. 49
Figure 4-12 Normalized Plot. 50

List of Tables

Table 3-1 Experimental Parameters: Set1 26

Table 3-2 Experimental Parameters: Set 2 27

Table 3-3 Experimental Parameters: Set 3 29

Table 3-4 Experimental Parameters: Set 4 31

Table 3-5 Experimental Parameters: Set 5 32

Table 3-6 Experimental Parameters: Set 6 34

Table 3-7 Experimental Parameters: Set 7, 8, 9 36

Table 3-8 Experimental Parameters: Set 10 37

Table 3-9 Experimental Parameters: Set 11 38

Table 4-1 Experimental Parameters for HoxB9 46

Chapter 1

Introduction

DNA (Deoxyribonucleic Acid) is a very fundamental and essential unit of life. It contains genetic and hereditary information. Each and every cell in a person's body has the same DNA. DNA is mostly found within the cell nucleus (Nuclear DNA) while some of it can be found in the mitochondria as well. The information in DNA is stored as a code made up of four chemical bases: Adenine (A), Guanine (G), Cytosine (C), and Thymine (T). An important property of DNA is that it can replicate, or make copies of itself. Each strand of DNA in the double helix can serve as a pattern for duplicating the sequence of bases. This is critical when cells divide because each new cell needs to have an exact copy of the DNA present in the old cell. An important function of DNA is coding for macro molecules, most of which are proteins but some are RNA molecules as well. Damage to the DNA at any location would mean stalling important processes like protein formation, cell replication etc. But the cell has an innate mechanism of fixing the damage. Thus DNA damage and its repair is a favorite research topic for researchers all over the world. If the cell is unable to fix the DNA damage, it leads to mutations in the genetic makeup of that cell or finally apoptosis (Programmed Cell Death). If the mutations persist, they may lead to early aging, due to genomic instability [5] or give rise to different types of cancers.

1.1 Cause of DNA Damage

Ionizing Radiation, Radiomimetic Chemicals, Collapsed Replication Fork [12], certain Endonucleases and Reactive Oxygen Species are all known to cause DNA damage. The most significant consequence of oxidative stress in the body is thought to be damage to DNA. Oxidative stress is caused by the presence of any of a number of reactive oxygen species (ROS) which the cell is unable to counterbalance. The result is damage to one or more biomolecules including DNA, RNA, proteins and lipids. Natural aging process is an implication of oxidative stress. DNA may be modified in a variety of ways, which can ultimately lead to mutations and genomic instability [49]. Ultraviolet and other types of radiation can damage DNA

in the form of DNA strand breaks. This involves a cut in one or both DNA strands; double-strand breaks are especially dangerous and can be mutagenic, since they can potentially affect the expression of multiple genes. UV-induced damage can also result in the production of pyrimidine dimers, where covalent cross-links occur in cytosine and thymine residues. The most common pyrimidine dimers are cyclobutane pyrimidine dimers (CPD) and pyrimidine (6-4) pyrimidone photoproducts (6-4PP). CPD and 6-4PP are the most frequent DNA mutations found in the p53 protein in skin cancers. Pyrimidine dimers can disrupt polymerases and prevent proper replication of DNA [49].

1.2 DNA Damage Repair Pathways

Cells cannot function if DNA damage corrupts the integrity and accessibility of essential information in the genome. DNA damage are recognized and processed by specific cellular response pathways [44][2] to ensure their efficient repair or, if the damage is too severe, apoptotic elimination of the cell occurs. Figure 1-1 shows the 5 known pathways of DNA Damage Repair that the cells undertake to process the repair based on the nature of DNA damage. Base Excision Repair (BER) is responsible primarily for removing small, non-helix-distorting base lesions from the genome. BER is important for removing damaged bases that could otherwise cause mutations by mispairing or lead to breaks in DNA during replication. BER is initiated by DNA glycosylases, which recognize and remove specific damaged or inappropriate bases, forming AP sites. These are then cleaved by an AP endonuclease. The resulting single-strand break can then be processed by either short-patch (where a single nucleotide is replaced) or long-patch BER (where 2-10 new nucleotides are synthesized). The related Nucleotide Excision Repair (NER) pathway repairs bulky helix-distorting lesions. NER is a particularly important mechanism by which the cell can prevent unwanted mutations by removing the vast majority of UV-induced DNA damage (mostly in the form of thymine dimers and 6-4-photoproducts). The importance of this repair mechanism is evidenced by the severe human diseases that result

from in-born genetic mutations of NER proteins including Xeroderma pigmentosum and Cockayne's syndrome.

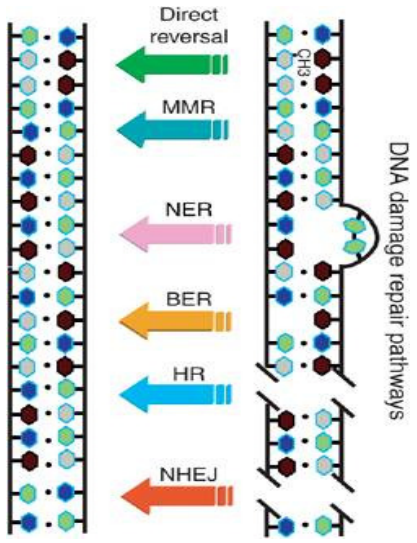

Figure 1-1 Different DNA Damage Repair Pathways

Non-Homologous End Joining (NHEJ) is a pathway that repairs double-strand breaks in DNA. NHEJ is referred to as "non-homologous" because the break ends are directly ligated without the need for a homologous template, in contrast to homologous recombination, which requires a homologous sequence to guide repair. NHEJ typically utilizes short homologous DNA sequences called micro-homologies to guide repair. These micro-homologies are often present in single-stranded overhangs on the ends of double-strand breaks. When the overhangs are perfectly compatible, NHEJ usually repairs the break accurately. NHEJ is evolutionarily conserved throughout all kingdoms of life and is the predominant double-strand break repair pathway in mammalian cells [23]. Homologous Recombination (HR) is a type of genetic recombination in which nucleotide sequences are exchanged between two similar or identical molecules of DNA. It is most widely used by cells to accurately repair harmful breaks that occur on both strands of DNA, known as double-strand breaks. HR is a high fidelity recombination process that leads to single strand stabilization and recombination occurs via homologous partner strand. The Single Strand Annealing (SSA) Pathway is a sub routine of the HR pathway.

1.3 Related Work

Laser microirradiation ranging in wavelength from ultraviolet A (UVA) to near-infrared (NIR) can be used to induce damage in a defined region in the cell nucleus, representing an innovative technology to effectively analyze the in vivo DNA double-strand break (DSB) damage recognition process in mammalian cells[8]. In their work on 'Comparative analysis of different laser systems to study cellular responses to DNA damage in mammalian cells' Kong, Mohanty et al. compared the nanosecond nitrogen 337nm UVA laser with and without bromodeoxyuridine (BrdU), the nanosecond and picosecond 532nm green second-harmonic Nd:YAG, and the femtosecond NIR 800nm Ti: sapphire laser with regard to the types of damage and corresponding cellular responses. The found different degrees of UV damage induced by different lasers and that ns UVA, ps green and fs NIR induce Cyclobutane Pyrimidine Dimers (CPD) and 6-4 Photoproducts (PP) whereas ns green generated some CPD but very little 6-4PP. Also Single Strand Breaks (SSB) are induced by different Lasers but base damage is induced by only high-dose UVA. Their findings show green and NIR lasers are suitable for detection of DSB factors but not for the formation of IRIF. Depending on their findings they came up with a flowchart of possible mechanisms of DNA damage.

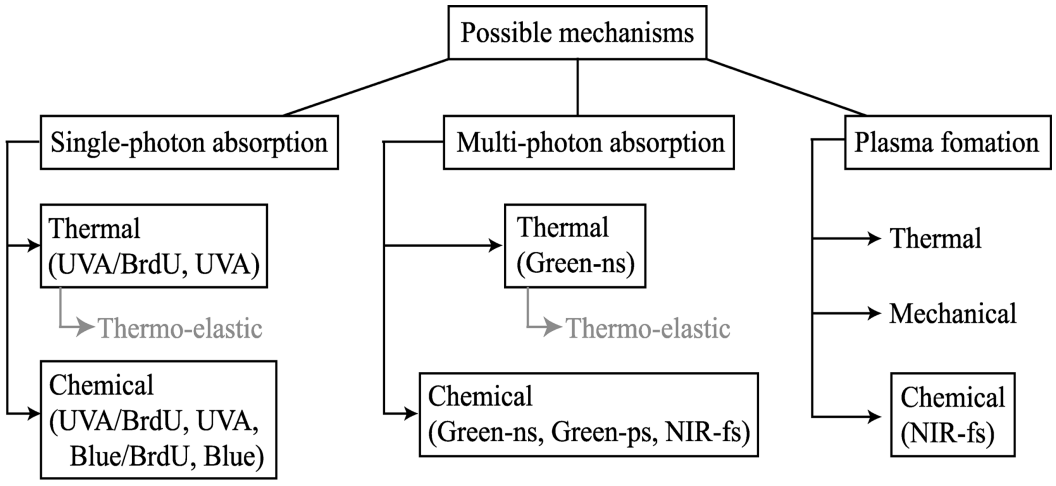

Figure 1-2 Possible Mechanisms of DNA Damage [8]

In our work we use an 800nm NIR laser and thus according to the above flow chart the damage induced by our system is a combined effect of multi-photon absorption as well as plasma formation which is mostly due to the high intensity laser beams used.

In another work, Mohanty, Rad et al [7] have shown the wavelength dependency of DNA damage. Over the wavelength range of 750 to 1064 nm, the amount of damage in DNA peaks at around 760 nm, with the fraction of DNA damage within the range of 750-780 nm being a factor of two larger than the fraction of DNA damage within the range of 800-1064 nm. The variation in DNA damage was not significant over the range of 800-1064 nm. The damage threshold values were fitted on two straight lines, one for continuous-wave sources and the other for pulsed source. The damage threshold around 760 nm fell on the line extrapolated from values for UV-radiation-induced damage, while the data for 800-1064 nm fell on a line that has a different slope. The change in the slope between 320 and 340 nm observed earlier is consistent with a well-known change in DNA-damaging mechanisms. The change observed around 780 nm therefore suggested a further change in the DNA damage mechanism.

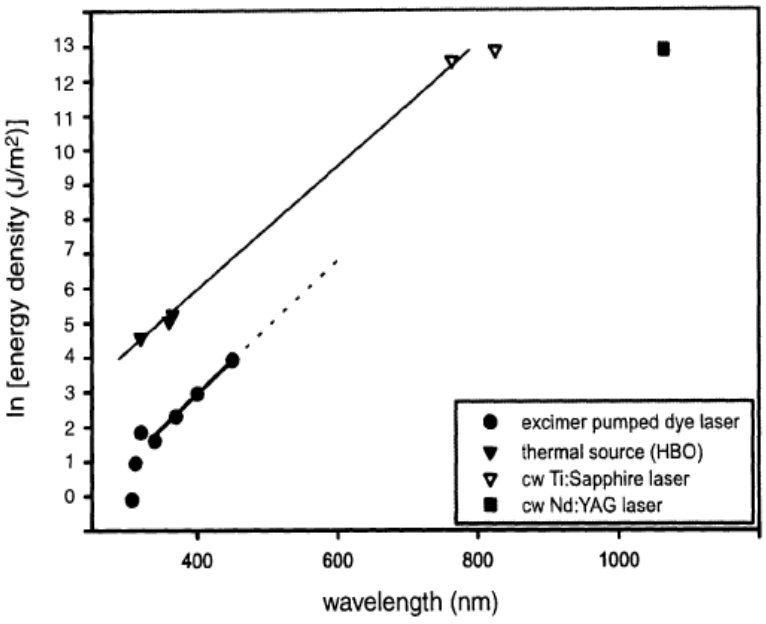

Figure 1-3 Wavelength Dependence of DNA Damage [7]

Semi-logarithmic plot of the minimum dose required to induce DNA damage above the control level using different light sources for irradiation. In the case of pulsed lasers, the dose required to observe DNA damage is lower than that due to continuous-wave light sources. The kink in the pulsed-laser data coincides with the well-known change in repair mechanisms from direct DNA damage to indirect. A kink on the continuous-wave laser data may indicate a change in mechanism of damage at approximately 780-800 nm [7]. This work also shows the energy density dependency of DNA damage. An increasing level of DNA damage was observed with increasing laser energy density. Also the quantity of DNA damage increased with increase in exposure. If the pulsed laser plot is extrapolated to 800nm to calculate the threshold energy density to induce DNA damage, it is observed to be in the order of $10^{\wedge 10}$. This is much lower than the energy density calculations of our system and can be due to the inherent sensitivity of the Comet Assay method of DNA damage detection used in the above study.

1.4 Motivation

We know that DNA is an important aspect of life and that any damage to the DNA, if not repaired can be lethal. Proper recognition and repair of DNA damage is critical for the cell to protect its genomic integrity[4][30]. Over the years, many researchers have dedicated their life in understanding every aspect of DNA damage and its repair right from the cause of DNA damage to how DNA damage can be induced to study the response of the cell. Such comprehensive studies have let to establishing markers or specific proteins that play a key role in DNA damage repair. For example, PARP-1 is a known marker for single strand break (SSB) where as γ-H2AX is an established marker for double strand DNA damage [21].

How would it be to search for new repair proteins that may play an important role in the entire DNA damage recognition pathway? This would provide us an opportunity to manipulate the process of DNA damage repair. This could help prevent mutations from being passed through generations, find a cure for cancer and also have an answer to the ever-looming

question of ‘Aging’. It is essential to study the protein extensively for parameters like accumulation time, which type of DNA damage triggers it, the effect of pulse energy on it.

With every passing day, there is a speculation of new proteins being involved, in their respective way, in the process of DNA damage recognition/ repair. It was observed by a group of researchers that MLL is amplified in some cancers and that it also responds to oxidative stress. It is known that a protein sub-unit of MLL-1, PTIP, plays a role in DNA damage repair/ response. PTIP, is also implicated in maintenance of genomic integrity [1][9][17]. PTIP is capable of interacting with DNA damage response proteins like 53BP1 and is also seen to be a component of SET domain HMT’s MLL-3 and MLL-4 and its other protein sub-units [19][36]. We began to wonder if MLL was involved in the DNA damage recognition/ repair pathway. MLL is amplified during gene transcription and is also a master box of Hox genes [24]. It is thus natural to speculate that if MLL plays a role in DNA damage recognition/ repair, HoxB9 could also be involved in the same.

By centering my study on some known factors and speculating their interaction with some unknown parameters, I have contributed my bit to the vast area of DNA damage-repair research. In the broad picture, if the involvement of a protein in the repair pathway is known, it can be chemically up-regulated or down-regulated (In vivo) to ensure DNA damage repair of every DNA break. This would eliminate chances of random mutations that cause cancer and increasing the longevity of life.

Chapter 2

Materials & Methods

2.1 Multimodal Setup

The Multimodal setup used in this experiment was built by the Biophysics and Physiology group under the guidance of Dr. Mohanty. The existing multimodal system includes Phase Contrast Microscopy (PCM), Digital Holographic Microscopy (DHM), Epifluorescence Microscopy, Atomic Force Microscopy (AFM), Near-Field Scanning Optical Microscopy (NSOM), Total Internal Reflection Microscopy (TIRFM) and Multiphoton Microscopy (MPM). In this study we have mainly made use of PCM, Epifluorescence Microscopy and MPM. A picture of the actual setup is shown in Figure 2-1:

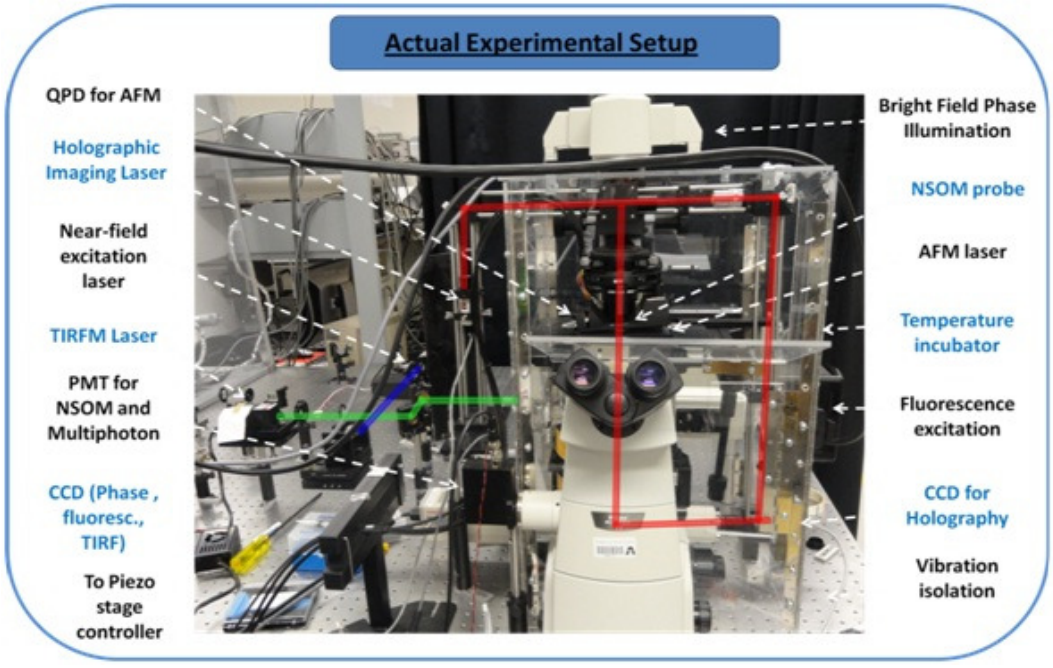

Figure 2-1 Multimodal Setup.

Principles of phase contrast imaging revolutionized optical microscopy by making it possible to visualize transparent specimens like live cells, thin tissue slices etc with high contrast [11]. The light passing through the sample lags the un-deviated light by ¼ of wavelength which results in poor contrast when the two beams arrive at the imaging plane. The set-up uses phase ring which allows the un-deviated light travel faster (shorter path length) and thus creating a phase difference of ½ wavelength which enables destructive interference and better contrast. A condenser is also used, which is adjusted to ensure maximum white light (from halogen light source) falls on the sample and objective, for better contrast. The sample is viewed using Phase 3, 100x 1.3 N.A microscope objective and imaged using Photometrics Coolsnap K4 CCD camera interfaced with the computer [11].

The application of fluorescence in microscopy for viewing biologically fluorescent samples did not come into being till the discovery of naturally fluorescent substances (fluorochromes), which were used in biological investigations. The basic function of a fluorescence microscope is to irradiate the specimen with a desired and specific band of wavelengths, and then to separate the much weaker emitted fluorescence from the excitation light. The fluorescence microscope in our set up is equipped with a high-intensity light source (a mercury arc lamp) that emits light in a broad spectrum from visible through ultraviolet. A special bandpass filter allows only a narrow band of emitted spectrum to pass through which then impinges on a dichroic beam splitter and is reflected through the objective lens and onto the sample [11]. The fluorochromes within the sample absorb the excitation light and emit a wavelength of light is characteristic of the fluorochrome. The filter turret has a combination of UV, Blue and Green excitation filters with Blue, Green and Red emission filters respectively. Thus a combination of Blue excitation with Green emission filter allows us to image GFP tagged molecules [11].

In the multimodal setup, a tunable Ti: Sapphire Laser, tunable from 690nm to 1040 nm with a pulse width of ~200 fs and a repetition rate of approximately 80 MHz is used. A tightly

focused laser beam at a high power can be used as “Laser Scissors’ to perform nano-surgery onto biological samples [11]. The laser is coupled to the microscope through an opening in the back and is reflected using a dichroic mirror to completely fill the back aperture of the objective. Before entering the microscope, laser beam was expanded using a set of two convex lenses and then made to pass through 1:1 telescope, shutter and polarizer before it entered into the microscope. 1:1 telescope enabled adjustment in focusing of the laser spot along axial direction, shutter was used to generate a pulse train when required while a polarizer enabled tuning of the power of laser beam.

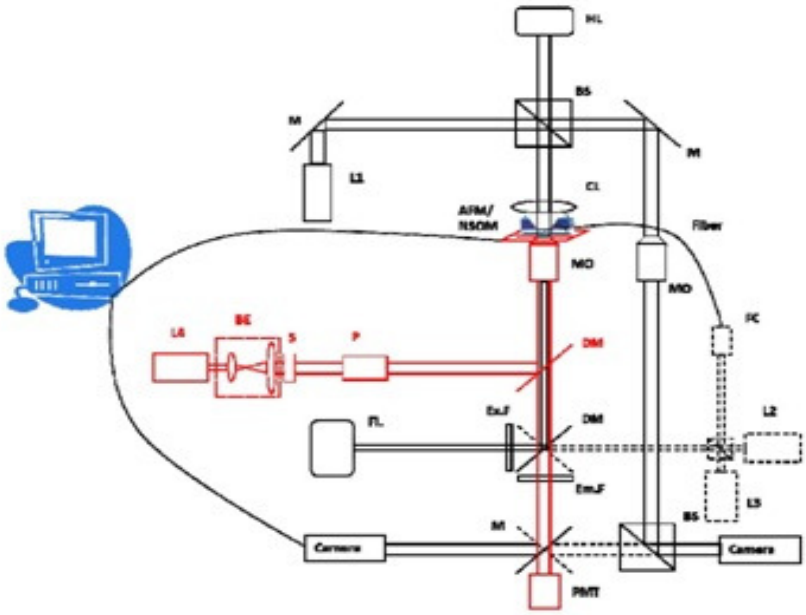

Figure 2-2 Schematic of the actual Multimodal Setup

2.2 Various Cell Lines

2.2.1 HeLa Cells

HeLa cells are the oldest and most common human cell line, used in scientific research. The line was derived from cervical cancer cells taken on February 8, 1951 from Henrietta Lacks, a patient who eventually died of her cancer on October 4, 1951. The HeLa cell line was derived for use in cancer research and was found to be remarkably durable and prolific as illustrated by

its contamination of many other cell lines used in research. These cells proliferate abnormally rapidly, even compared to other cancer cells. HeLa cells have an active version of telomerase during cell division, which prevents the incremental shortening of telomeres that is implicated in aging and eventual cell death. This way the cells circumvent the Hayflick Limit, which is the limited number of cell divisions that most normal cells can later undergo before becoming senescent. Hence it is an immortalized cell line. An image of HeLa cells is shown in Figure 2-3

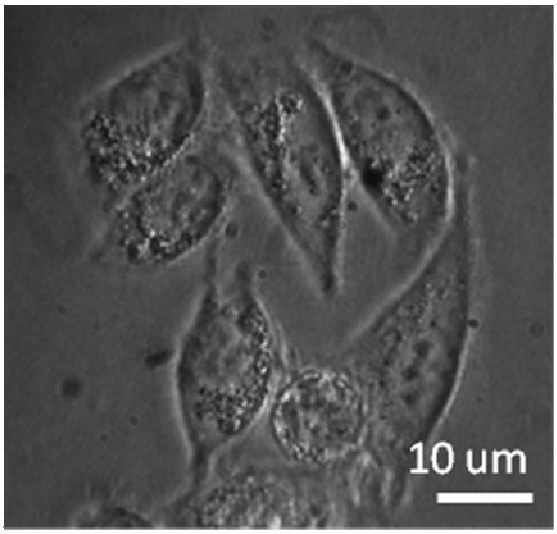

Figure 2-3 HeLa Cells

2.2.2 HEK 293 Cells:

Human Embryonic Kidney 293 cells, also often referred to as HEK 293, 293 cells, or less precisely as HEK cells are a specific cell line originally derived from human embryonic kidney cells grown in tissue culture. HEK 293 cells are very easy to grow and transfect very readily and have been widely-used in cell biology research for many years. HEK 293 cells were generated in the early 70s by transformation of cultures of normal human embryonic kidney cells with sheared adenovirus 5 DNA in Alex van der Eb's laboratory in Leiden, The Netherlands. The human embryonic kidney cells were obtained from a single apparently healthy fetus legally aborted under Dutch law. As an experimentally transformed cell line, HEK 293 cells

are not a particularly good model for normal cells, cancer cells, or any other kind of cell that is a fundamental object of research. However, they are extremely easy to work with, being straightforward to culture and to transfect. In our experiments we use HEK cells in which the HoxB9 gene is over expressed and tagged with a Green Fluorescent Particle (GFP), provided by our collaborator, Dr. S Mandal, The University of Texas, Arlington. Figure 2-4 shows an image of a cluster of HEK cells (L) shows a single fluorescent HEK cell.

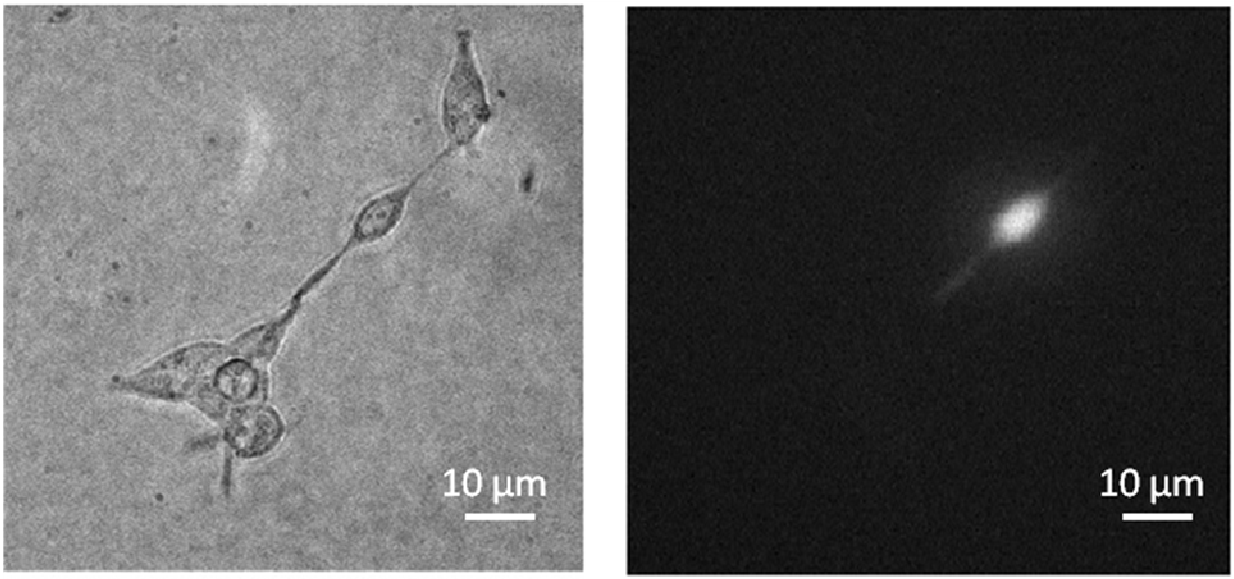

Figure 2-4 HEK 293 Cells. (L) Bright Field Image (R) Fluorescent Image

2.2.3 HT1080 Cells

HT1080 is a human fibroblast cell line which has been used extensively in biomedical research. The cell line was created from tissue taken in a biopsy of a fibrosarcoma present in a 35 year old human male. The patient who supplied the sample had not undergone radio or chemotherapy and this lack of therapy is important as both radio and chemotherapy may introduce unwanted mutations into the sample. We have worked with HT1080 cells in which the TRF2 is Yellow Fluorescent Particle (YFP) tagged. These cells were provided by Dr. Giley's lab from Indiana University School of Medicine, Department of Radiation Oncology, Indianapolis, Indiana. TRF2 stands for Telomeric Repeat-binding Factor 2 and is known to play a significant

role in telomere maintenance and thus are said to be involved in DNA damage recognition/ repair pathway. Figure 2-5 shows the immunofluorescence imaging of a HT 1080 cell post DNA damage showing TRF2 accumulation at the damage site.

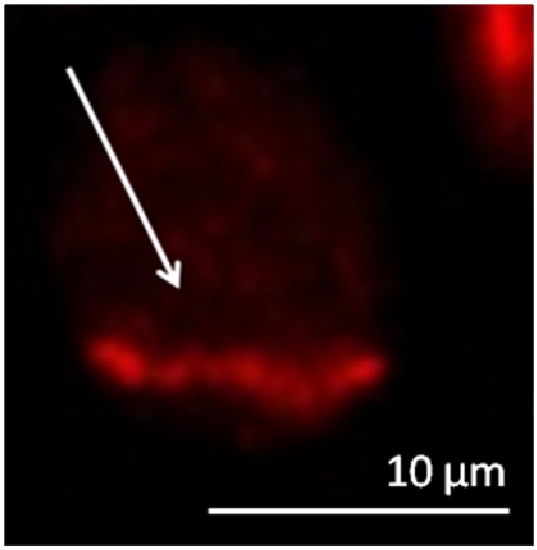

Figure 2-5 HT1080 cells with TRF2 antibody staining

2.3 Cell culture

Thawing the preserved cells is the first and the foremost important step for this study. In order to maintain a constant supply of healthy cells for experiments, it is essential that the cell culture must be carried out under proper cell culture conditions in a Bio-safety hood, to prevent unwanted contamination. Cells were grown in cell culture flasks containing growth media till they are almost 50% confluent. The growth media consisted of Advanced DMEM (Invitrogen Corp., CA, USA) supplemented with 10% fetal bovine serum. Once they reach the desired confluence they were further sub-cultured into smaller petri dishes and used for experiments. These petri dishes are cover-slip bottomed and coated with Poly-d-Lysine to ensure the cells attach and grow in the dish. The cells in the flask were dislodged using Trypsin. These cells, suspended in a mixture of growth media and Trypsin, were centrifuged for 5 minutes at the speed of 3000 rpm. This separated the cell palette from the liquid which was discarded. The

cells were re-suspended in fresh media and plated for experimental use. The HEK-HoxB9-Over-expressing-GFP and HT1080-TRF2-YFP cells were cultured in a similar way except that the media for these cells contained G418, an antibiotic used for transfected cells. All cells were cultured in cell culture CO_2 incubator at 37˚C in an atmosphere of 5% CO_2.

2.4 Marking Region of Interest (ROI) on the dish

The cover-slip bottomed petri dishes used were 35mm (diameter) dishes from MatTek Corporation. The microwell area where the cells attach was approximately 14mm in diameter. At the bottom of all dishes, in the microwell region, a small dot was made on using a permanent marker. This helped in locating healthy cells around the dot and in the imaginary 4 quadrants, for which the dot was the origin.

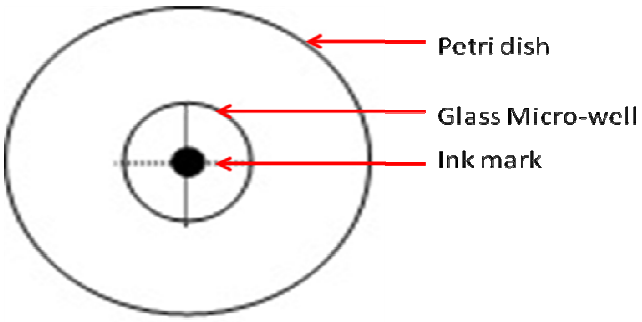

Figure 2-6 Marking the ROI.

2.5 Induction of localized DNA damage with the use of laser

HeLa cells were plated in the cover-slip bottomed dish and once they were 50% confluent they were ready for experimentation. The dishes were removed from the incubator and placed in a closed chamber around the sample stage. We tried to maintain a certain level of humidity in the chamber. As we used the 100x 1.3 N.A oil emersion objective, a drop of oil was placed on the objective before placing the Petri dish. The cells were first viewed using the 'Eye' port of the microscope to be able to focus better. Care was taken while focusing on the cells,

not to trap any bubble between the oil drop and the bottom of the dish. The presence of oil drop, if any, made it difficult to focus clearly on the cells by continually varying the focal plane. Once the cells were focused, we checked for the laser beam. For DNA damage experiments it is essential to use the laser which is pulsing and with Mode Locker 'ON'. To ensure the laser was pulsing throughout the experiment, the shutter in the beam path must remain open and the polarizer setting must be appropriate so that the beam has enough power to cause DNA damage but not kill the cell. The power of the laser beam was measured using a power meter placed at the back aperture of the objective. The power reading was then multiplied by the transmission factor at that particular wavelength (0.6 at 800 nm) to obtain the actual power reading. The power level recorded at the power meter was ~150 mW before the objective. The effective power after the objective is ~ 80mW. Depending on the exposure time of the laser pulse (20 msec) much lower power actually reaches the cells.The Mai-Tai controller GUI is shown in Figure 2-7 using which we were able to control the pulsing of the laser, actuate the shutter and also control the power level. By opening all the apertures in the laser beam pathway, the beam profile was checked (Laser at a very low power level and not pulsing) and was adjusted using the X-Y micromanipulators at the back of the microscope. The laser beam was adjusted till the pattern as shown in Figure 2-8 was observed. The laser beam size of our setup is of the order of 800 nm.

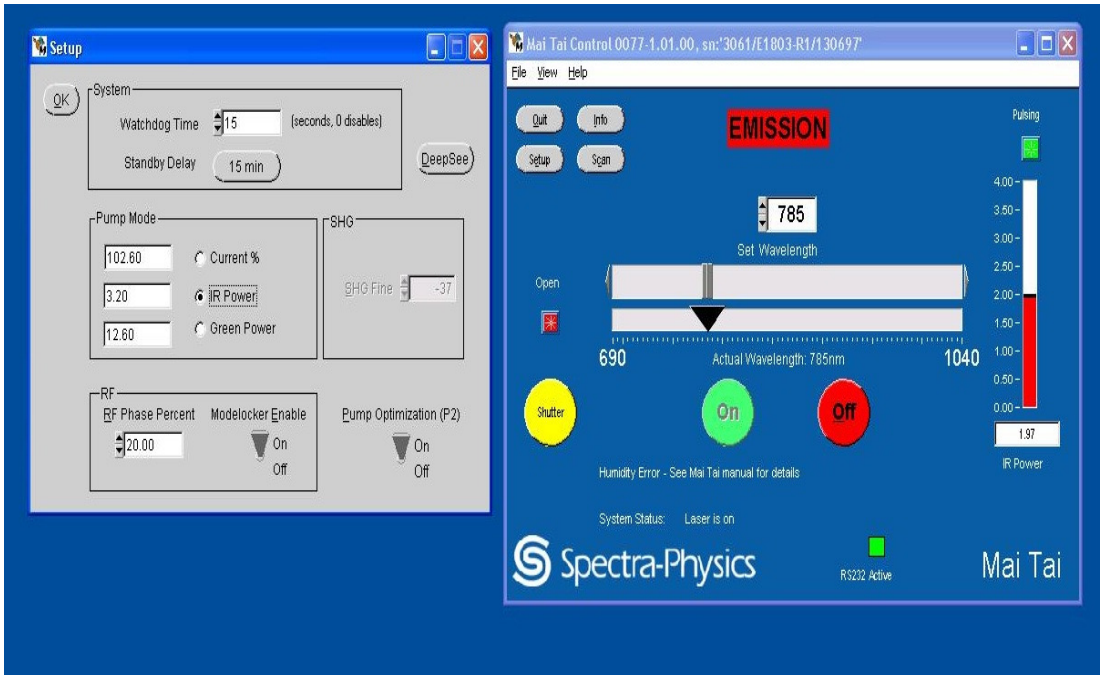

Figure 2-7 Mai Tai Controller GUI

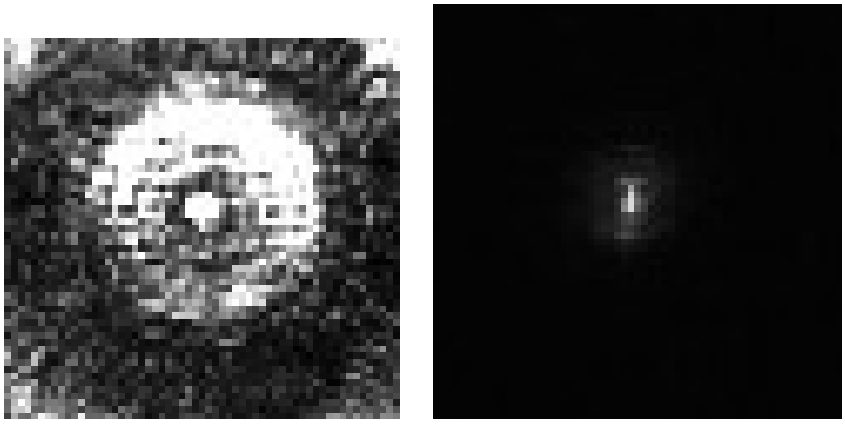

Figure 2-8 Laser beam Profile (L) Unfocused Beam (R) Focused Beam spot.

From an external controller, the laser can be controlled via a shutter. This controller also allows one to use the laser in a pulsed or continuous mode and also set the exposure and delay timings, over the range of µsec to seconds, as per requirement. The microscope is then shifted from the 'Eye' port to the 'Left' port which has the camera. The sample is viewed on the

computer using PM Micromanager (shown in Figure 2-9) which can be used to change the exposure of the camera as per requirement and also allows choosing between snapshot images or multiple acquisitions. Using the 'Live' mode, the cells are focused to a point where the nucleus (dark region within the cell) is clearly visible. The laser is actuated in a pulsing mode from the external controller and using the sample stage X-Y manipulator, the cells were moved in the field of the laser beam so as to cause DNA damage. Since the manipulation is manual, it is not always accurate and does not have a fixed pattern of damage.

Figure 2-9 PM Micromanager GUI.

2.6 Immunostaining

Following the laser-induced DNA damage, the next step was to fix the cells and stain them. The total time for which the entire dish was exposed to laser irradiation was ~ 10 minutes (This time depends on the number or cells irradiated per dish; individual cells are exposed to the laser for much less time) The cells are allowed to sit for a few minutes before being fixed ($t_{|fix}$) and it is hypothesized that it is within this time that the cells recruit DNA damage recognition/ repair proteins. However it must be noted that different proteins have their

respective response time. Cells from different sets of experiments were fixed at different times to investigate the possible effect of varying the fixing time ($t_{|fix}$). At the end of $t_{|fix}$, growth media is aspirated from the dish and the cells are fixed with 4% Paraformaldyhyde (PFA) for 15 minutes. Fifteen minutes later, the dish was rinsed with 1x PBS (Phosphate Buffered Saline) 3 times for 5 minutes each. This was followed by primary and secondary anti-body staining. After rinsing with 1x PBS cell fixation, we added the Blocking Buffer consisting of 1% Bovine Serum Albumin (BSA), 2% Goat Serum in 1x PBS, approximately 100-200 µl/-dish for 45 minutes at room temperature. The function of blocking buffer, as the name suggests, is to block any residual sites to prevent non-specific binding of anti-bodies.

At the end of 45 minutes, the Blocking Buffer was aspirated and the cells were stained with the Primary Antibody + 1% BSA in 1x PBS for 1-2 hours. Different primary anti-bodies are used to screen for different proteins as discussed later. For a successful immunostaining, the Primary and the Secondary anti-body must be compatible and while staining for 2 different proteins, they must excited by different excitation light under the fluorescence microscope and must have well separated emission spectra. The primary anti-body is aspirated from the dish and rinsed with 1x PBS 3 times for 5 minutes each. Similar to the Primary antibody, the Secondary anti-body + 1% BSA in 1x PBS was added for 1-2 hours and rinsed with 1x PBS at the end of staining time. The next step was staining with Hoechst 33258, which is a dye used to stain the nucleus of fixed cells. 100µl of Hoechst (0.12 µg/ml conc.) was added to the micro-well in the dish and kept for an additional 15 minutes at room temperature. The dish was rinsed at the end of 15 minutes with 1x PBS (3 times) to remove any residual dye. Hoechst is mainly used to stain the DNA present in the nucleus, which is clearly seen with fluorescence imaging and helps in image analysis when a composite image is formed, using ImageJ (described later in 2.9 Software: ImageJ)

2.7 Imaging of Immunostained Cells

In order to image the immunostained cells, we used Fluorescence Microscopy. The white mercury lamp needs to warm up for ~2 minutes before it can be powered on. The petri dish is placed on the sample stage and focused on the imaging plane. The irradiated cells are located with the help of the reference dot and a bright field image is first captured under the halogen light using PM micromanager. Since the fluorescence is a low level phenomenon, the camera exposure was adjusted between 200-500µsec. Also the neutral density filters ND4 and ND8 were in place to avoid bleaching the sample. The nuclear staining with Hoechst is visible with filter #1 (UV excitation; Blue emission), proteins in green are seen with filter #2 (Blue excitation; Green emission) and proteins in red are seen with filter #3 (Green excitation; Red emission).

2.8 Induction of DNA damage by ultrafast laser microbeam and live imaging

The cells used for live imaging were HEK-HoxB9-Over-expressed-GFP tagged cells. The cells were placed on the sample stage and viewed with a 100x 1.3 N.A objective (Oil Immersion Objective) as described earlier. This technique required the Ti: Sapphire laser to be focused on the nuclei of a fluorescent cell to be able to cause point damage while simultaneously acquiring multiple images of the cell to analyze the change in fluorescence. Both the halogen and mercury lamps were utilized for bright-field and fluorescent images respectively. A healthy fluorescent cell is spotted in the ‘Eye’ mode of the microscope and a single laser beam pulse (Exposure time can be varied) was given using the external controller. The camera was made to acquire images before the pulse was applied and went on for 300 seconds at the rate of 1frame/sec. In case of a few cells we were required to give more than one pulse and these pulses correspond with the peak in intensity levels seen on analyzing these images. The image sequence is analyzed in ImageJ by comparing the integrated image densities around the laser beam and in a control area in the same cell.

The HT1080-TRF2-YFP cells were also imaged simultaneously with laser induced DNA damage, in the same way as the HEK-HoxB9-Over-expressed-GFP cells, for the kinetics study. In this case, we studied the accumulation of TRF2 at the site of DNA damage, over time. To analyze the dynamics of TRF2 diffusion, we used a 405nm UV laser in the Confocal Microscope on cells that were pre-sensitized with Hoechst 33342.

2.9 Software: ImageJ

ImageJ is the software used for analyzing the images. It is a Java-based image processing software developed by NIH, which already had in-built functions for basic image processing tools and also allows the user to develop their own plugins. For processing the immunofluorescence data, the raw image files are opened in ImageJ and set to the respective channels using the look-up color tables. The brightness and contrast are adjusted so as to be able to clearly view accumulation of proteins, if any. To form a composite image, the user is required to select the correct data file for each color channel (4 Channels: Grey, Blue, Green and Red). Any of the fields may be left blank if the image of that channel is unavailable.

For analyzing the fluorescence time-lapse images, an entire image sequence is imported in ImageJ. The cell of interest is located and in that cell 2 spots are cropped: one around the laser spot and another control from any other part in the cell. The integrated intensity of each spot over all the frames is calculated using the inbuilt function. The results are available in Microsoft Excel format which can be saved and worked with later.

Chapter 3

Fixed Method

The experiments to study the involvement of repair proteins from the Mixed Lineage Leukemia (MLL) family and the Homeobox (Hox) domain can be broadly classified in 2 categories: 1. Direct method which is based on immunostaining of proteins and 2. Indirect Method where we observed the fluorescence time-lapse of proteins hypothesized to be involved. Both methods have their own advantages and shortcomings. The immunofluorescence of proteins screened by the Direct method is high and accumulation of proteins at the DNA damage site is clearly visible but the fixing time ($t_{|fix}$) is fixed for each experiment set. With each set of experiment, we varied $t_{|fix}$ to investigate a possible time-dependence. In the Indirect method, we can acquire time-lapse images for a much longer time but the low fluorescence of the transfected cells is a trade-off. An overview of the experimental approach is shown in the flow-chart below.

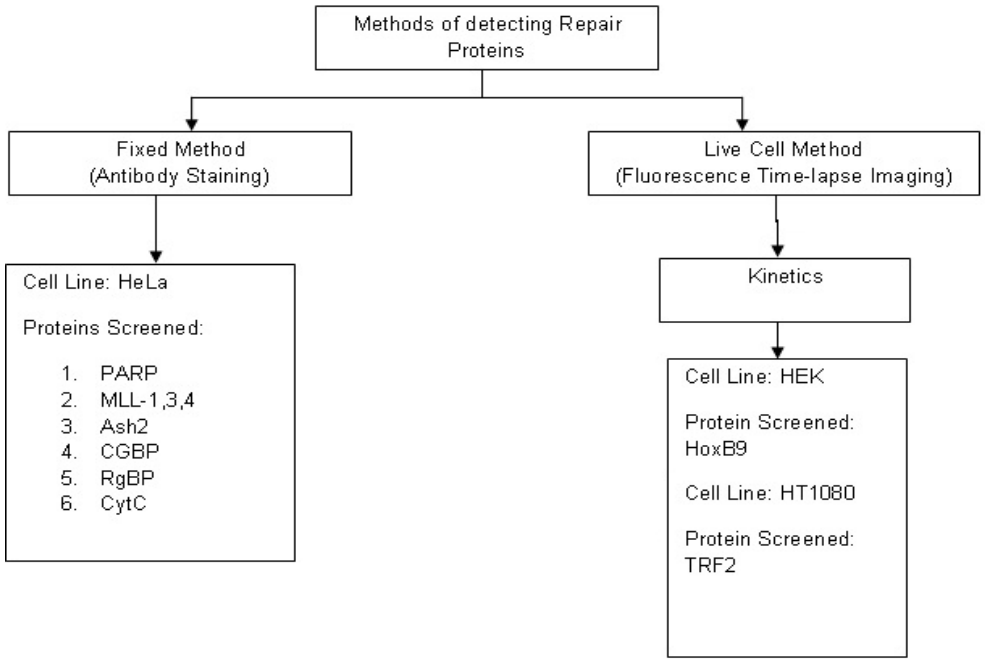

Figure 3-1 Experimental Flow-chart

3.1 Poly ADP Ribose Polymerase (PARP)

Poly(ADP-ribose) polymerase (PARP, EC 2.4.2.30) is a highly conserved enzyme that catalyses the addition of ADP–ribose polymers from NAD^+ to a variety of protein substrates, including itself and other nuclear proteins [43]. PARP participates in the intricate network of systems developed by the eukaryotic cell to cope with the numerous environmental and endogenous genetoxic agents [43]. PARP can be associated with sub-cellular components other than the nucleus, and may indicate additional roles for this enzyme [35]. PARP is strongly activated by DNA strand breaks, and it has been suggested that PARP is primarily involved in facilitating the access of repair enzymes to damaged DNA [39]. DNA strand breaks, generated either directly by genotoxic agents (oxygen radicals, ionizing radiations, or monofunctional alkylating agents) or indirectly after enzymatic incision of a DNA-base lesion, trigger the synthesis of poly(ADP-ribose) by the enzyme poly(ADP-ribose) polymerase (PARP [E.C.2.4.2.30]) [34]. PARP is associated with the nuclear matrix [3] and [42], and specifically with the nucleolus [42] in cultured cells. It has already been established that PARP is involved in DNA damage repair as PARP activity is stimulated > 500-fold on binding to DNA strand breaks [34]. Also Javier et al. have indentified XRCC1 (X-Ray-Cross-Complementing-1) which is involved in the Base-Excision Repair (BER) pathway, as a partner of PARP [34]. The involvement of PARP in DNA damage repair has been verified in PARP-deficient cells which on investigation demonstrate the absence of the polymerization step for the BER pathway [34]. Also in the absence of PARP, when un-repaired DNA damage is encountered during DNA replication, the replication is stalled and there is an evident increase in Homologous Recombination pathway [32][33][40]. Figure 3-2 depicts the activation pathways of PARP upon DNA damage. Depending on the extent of DNA damage, PARP can either activate an ATM, DNA-PK or p53 based responses which lead to any of the 3 possibilities: 1. DNA repair, 2. Cell Cycle Arrest, 3. Apoptosis. A high extent of damage will lead to the activation of NAD+ pathway leading to necrosis.

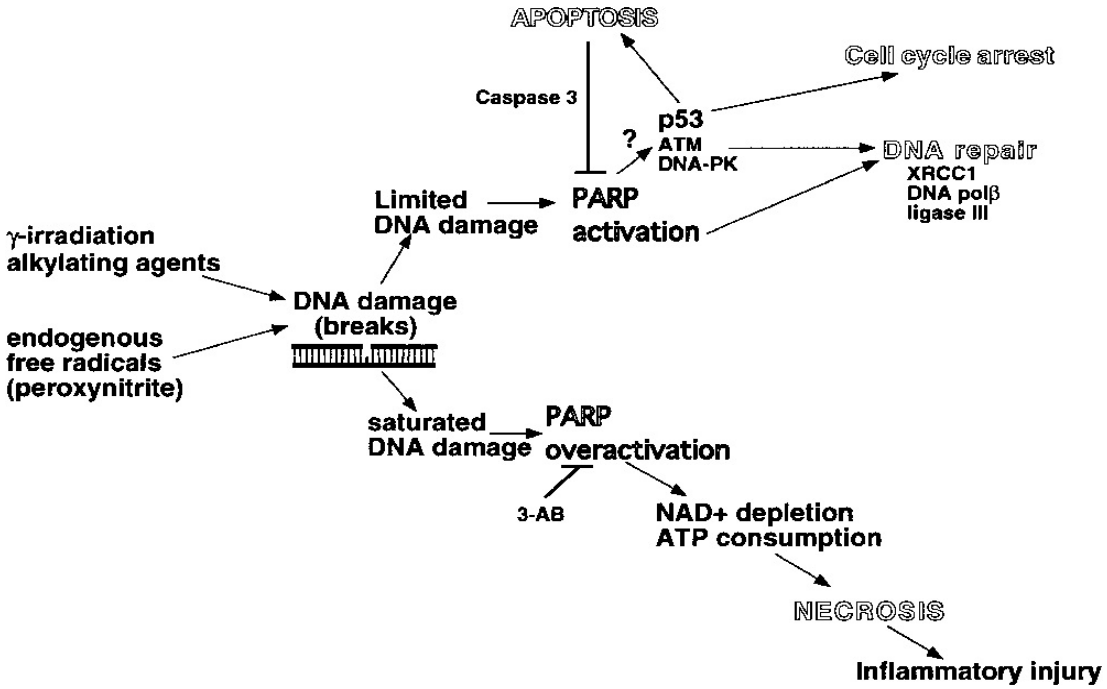

Figure 3-2 PARP Response Pathway

3.2 Mixed Lineage Leukemia (MLL)

Mixed Lineage Leukemia (MLL) is a gene that codes for the enzyme Histone-lysine N-methlytransferase HRX [22] and is involved in the epigenetic maintenance of transcriptional memory and pathogenesis of human leukemia [14]. MLL is a histone methyltransferase deemed a positive global regulator of gene transcription [26][27]. Histone lysine methylation is a prominent posttranslational modification linked to diverse biological pathways including gene transcription (Martin and Zhang, 2005), maintenance of heterochromatin (Lachner et al., 2001; Schotta et al., 2002) and double-stranded DNA break repair [41]. MLL's are also associated with cancer [28]. Set1 families of enzymes which include MLL 1-5 are mainly responsible for H3K4 di/trimethylation in vivo [41]. Also Set1 families are associated with multisubunit protein complexes, the common 3 of which are Ash2L, WDR5 and RbBP5 and in this study we have tried to study the interaction of Ash2L and RbBP5 with MLL-1 upon induction of DNA damage. The work done by Dou et al [38]., 2006; Steward et al [29]., 2006; Wysocka et al., 2005 [47] has

already shown that the role of the subunits in regulating MLL-1 methyltransferase activity is shown by interfering with the function of the subunits, which ultimately leads to the loss of H3K4 trimethylation.

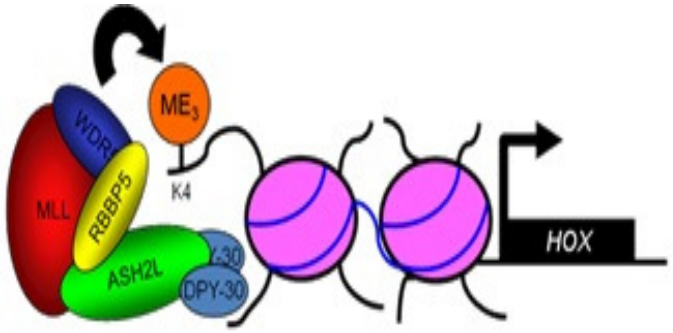

Figure 3-3 Structure of MLL and associated protein sub-units

ASH2L (Abscent, Small, or Homeotic-Like) encodes the protein ASH2L which is named after the Drosophila protein Ash2, a known regulator of HOX genes (Ikegawa et al. 1999) ASH2l is known to be a component of histone H3 lysine 4 (H3K4) methyltransferase complexes and H3K4 methylation is commonly associated with active gene transcription (Ikegawa et al. 1999; Huges et al. 2004; Dou et al. 2006; Steward et al. 2006; Cho et al. 2007). Previous studies have shown that disruption of ASH2L leads to a decrease in H3K4 trimethylation, which negatively affects gene expression (Dou et al. 2006; Steward et al. 2006). Furthermore, disruption of ASH2L or the methyltransferase involved in H3K4 methylation can lead to oncogenesis mostly through the regulation of Hox gene expression (Huges et al. 2004; Luscher-Firzlaff et al. 2008). Interestingly, overexpression of ASH2L leads to tumor proliferation and knockdown of ASH2L inhibits tumorigenesis, which is the reason why ASH2L leads to tumor prolification and knock-down of ASH2L inhibits tumorigenesis, which is the reason why ASH2L is thought to be an oncoprotein [45]. Understanding the role that ASH2L plays in facilitating proper H3K4 methylation may provide insight into how disruption of ASH2L can lead to abnormal cell proliferation and oncogenesis [48]. Furthermore ASH2L containing methyltransferase complexes are shown to be

important for the maintenance of HOX gene expression by binding to HOX gene promorters and by adding H3K4 di and trimethylation (Huges et al. 2004; Tan et al. 2008; Yates et al. 2010). HOX gene expression is important for proper development and differentiation, and disruption in H3K4 methylation leads to defects in HOX gene expression and the development of cancer (Tan et al. 2008; Hess, 2006; Rampalli et al. 2007; MacConaill et al. 2006; Huges at al. 2004).

Retinoblastoma-binding Protein 5 (RbBP5) plays a crucial role in embryonic stem cells in the differentiation potential, particularly along the neural lineage, regulating gene induction and H3 'Lys-4' methylation at key developmental loci, including that mediated by retinoic acid. As part of the MLL1/MLL complex, involved in mono-, di- and trimethylation at 'Lys-4' of histone H3. Histone H3 'Lys-4' methylation represents a specific tag for epigenetic transcriptional activation [50].

CpG Binding Protein (CGBP) in humans is encoded by CXXC1 gene and is known to regulate gene expression [6]. The work done by Ansari et al. 2007 shows CGBP is co-purified with three H3K4 specific HMTs MLL1, MLL2, and hSet1. They also performed independent immuno-precipitation of MLL1, MLL2 and hSet1 complexes from human cell and demonstrated that each of these complexes contains CGBP. In addition, CGBP is co-localized with MLL1, MLL2 and hSet1 in vivo and binds to the promoter of MLL target gene *HoxA7*. Antisense mediated knock down of CGBP diminished the recruitment of MLL1 and down regulated levels of H3K4 trimethylation in HoxA7 promoter affecting its expression. These results demonstrated that CGBP interacts with MLL1, MLL2 as well as hSet1 HMTs and plays critical roles in regulations of MLL target genes [18][25][26].

As mentioned earlier histone lysine methylation marks transcriptional activation. RNA polymerase II is present near the transcriptional site and is phosphorylated at the Ser 5 of its C-Terminal Domain (CTD). MLL-1 complex binds to Ser 5 of CTD and induces H3K4 me3 as well as acetylation of H4 [13]. Cytochrome C is believed to play a part in apoptosis. Hence we

investigated the interaction of CytC and MLL-1 if it was hypothesized that the laser-induced DNA damage lead to cell apoptosis.

3.3 Results

For all the experiment sets, λ is the laser wavelength (nm); t_{ex} and t_{del} are the exposure time and delay time for the laser pulse; t_{exp} stand for the total experimentation time and t_{fix} is the total fixing time. The figure shown alongside is schematic of the petri dish microwell, the solid black being the reference spot and the red being laser-induced DNA damage sites.

3.3.1 Experiment Set 1

Table 3-1 Experimental Parameters: Set1

λ = 800nm	Power = ~80mW
t_{ex} = 20 msec	t_{del} = 10 msec
t_{exp} = 10 min	t_{fix} = 5 min

In our 1st set, we screened for PARP and MLL-1. The PARP anti-body (Santacruz Biotech, Rb) was raised in rabbit and has a red emission where as the secondary anti-body was anti-rabbit, tagged with rhodamine (Red). The MLL-1 anti-body used had green emission. The images show the immunoflurescence of DAPI, MLL and PARP antibody. The laser induced DNA damage lines are clearly visible PARP staining where as they are only faintly visible in MLL-1 staining (Row 2, Column 3). PARP, a known repair protein for DNA damage repair, verifies the presence of DNA damage but MLL-1 is not co-localized with it. In Figure 3-4, (a) DAPI staining, (b) MLL-1, (c) PARP, (d) Post Irradiation and (e) Composite Image.

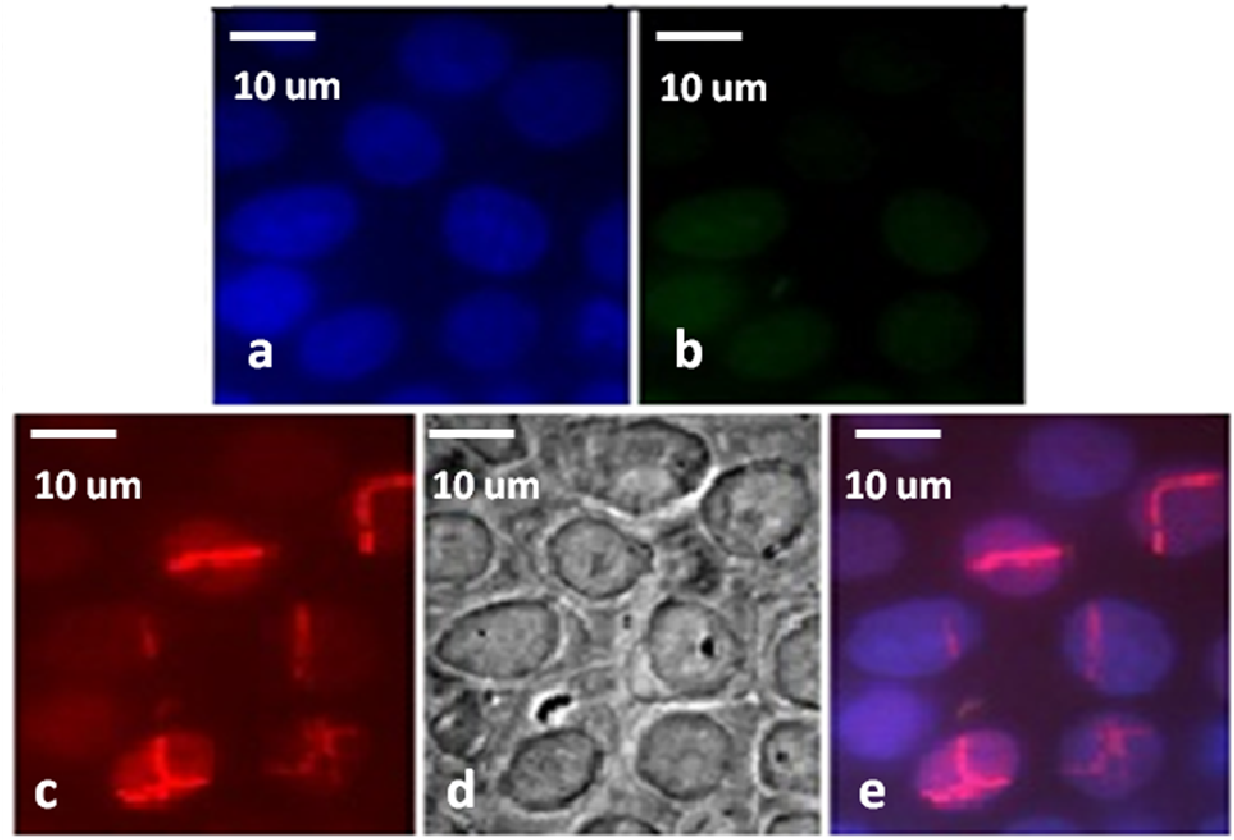

Figure 3-4 Results for MLL-1 (Green) and PARP (Red)

3.3.2 Experiment Set 2

Table 3-2 Experimental Parameters: Set 2

λ = 800nm	Power = ~80mW
t_{ex} = 20 msec	t_{del} = 10 msec
t_{exp} = 10 min	t_{fix} = 5 min

In this set of experiments, we screened for MLL-1 and ASH2. The MLL-1 (Mouse antibody) is seen in green and ASH2 (Rabbit antibody) is in red. In trial 1 (Row1, Column 4) we observe blackening of the cell membrane due to high intensity laser exposure. Also in the same

trial, we observe some positive staining in MLL-1 but none in ASH2. On creating a composite image using DAPI, MLL-1 and ASH2 in the Blue, Green and Red channels respectively, we find majority of the MLL-1 staining outside the nucleus. This accumulation of MLL-1 in the regions of heavy DNA damage is likely to be due to oxidative stress. In Figure 3-5, (a) shows nucleus of HeLa cells stained with DAPI (nuclear stain), (b) MLL-1 staining of the same cells, (c) Ash-2 staining, (d) Post Irradiation image of the same area and (e) Composite Image formed by superimposing images a, b & c

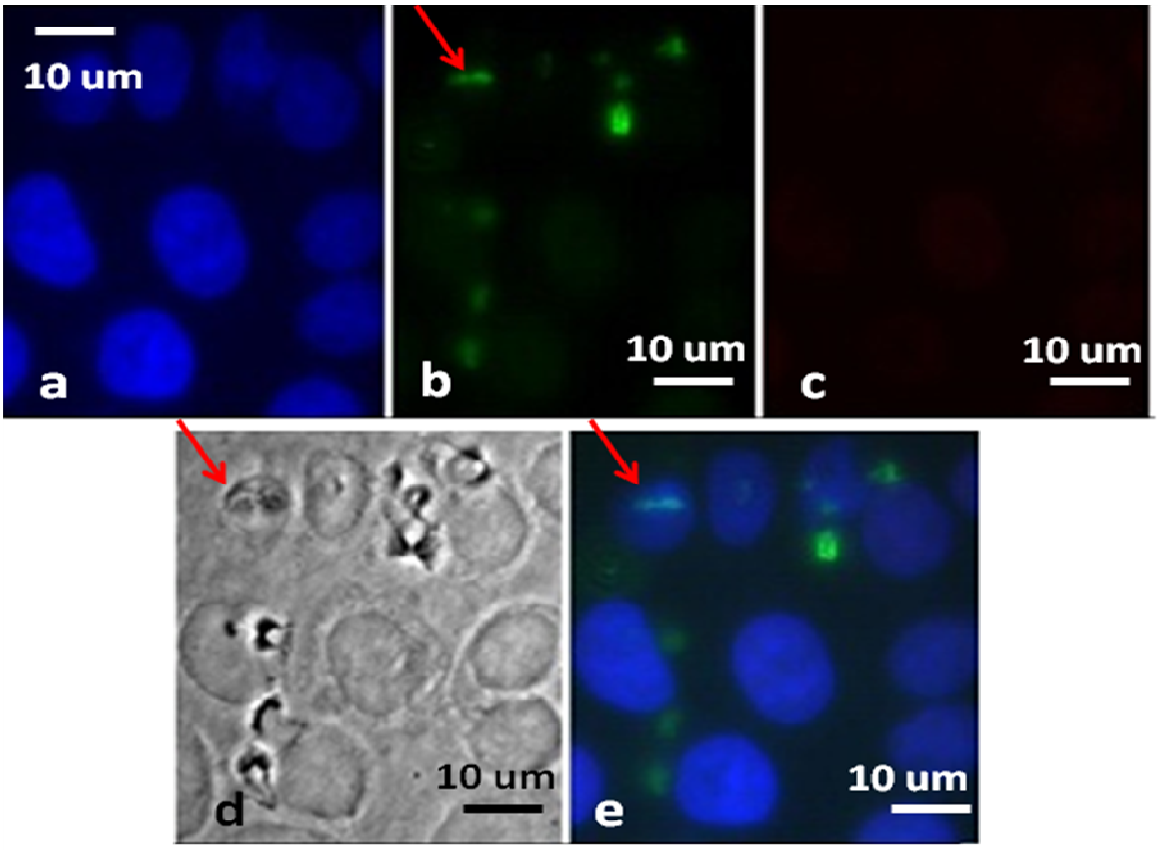

Figure 3-5 Results for MLL-1(Green) & Ash-2(Red).

3.3.3 Experiment Set 3

Table 3-3 Experimental Parameters: Set 3

λ = 800nm	Power = ~80mW
t_{ex} = 20 msec	t_{del} = 10 msec
t_{exp} = 10 min	t_{fix} = 10 min

The antibodies used for this set of experiments is MLL-1 (Mouse Antibody) in green and CGBP in green. The bright-field image shown in Row1, Column 4 carries evidence of high-level damage at the edge of the cell. The nucleus as shown in the DAPI staining is undamaged. The positive staining in MLL-1 and CGBP channel are due to oxidative stress. Trail 2 shows some faint, almost negligible staining in MLL-1. In Figure 3-6, (a) shows nucleus of HeLa cells stained with DAPI (nuclear stain), (b) MLL-1 staining of the same cells, (c) CGBP staining, (d) Post Irradiation image of the same area and (e) Composite Image formed by superimposing images a, b & c

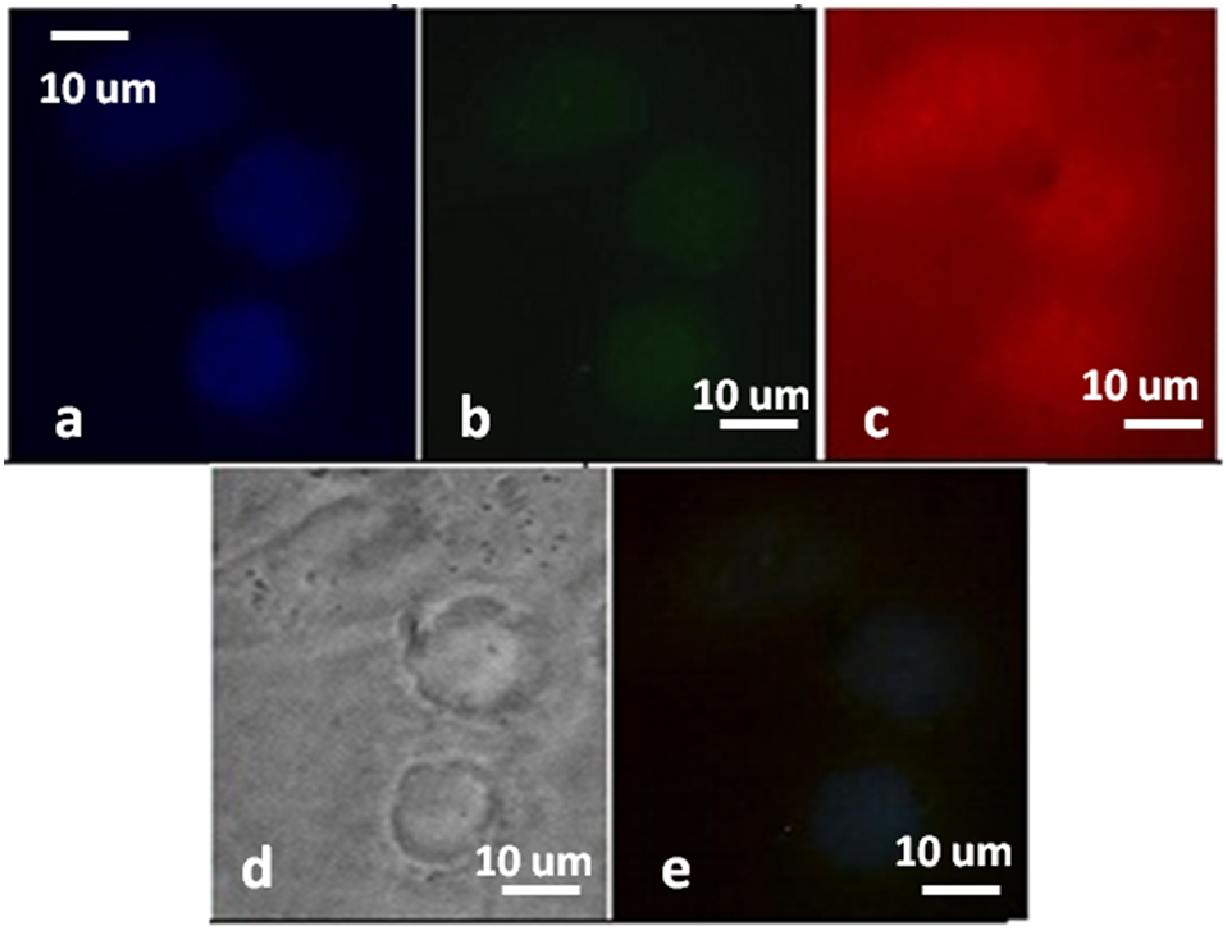

Figure 3-6 Results for MLL-1 (Green) and CGBP (Red).

3.3.4 Experiment Set 4

Table 3-4 Experimental Parameters: Set 4

λ = 800nm	Power = ~80mW
t_{ex} = 20 msec	t_{del} = 10 msec
t_{exp} = 10 min	t_{fix} = 10 min

The anti-body used for CTD (Rabbit antibody) is anti-RNA polymerase 2 and is seen in the red channel. The DNA damage line is faintly visible in the post-damage bright-field image but no accumulation is visible in the MLL-1 or CTD channel. In Figure 3-7 (a) shows nucleus of HeLa cells stained with DAPI (nuclear stain), (b) MLL-1 staining of the same cells, (c) CTD staining, (d) Post Irradiation image of the same area and (e) Composite Image formed by superimposing images a, b & c

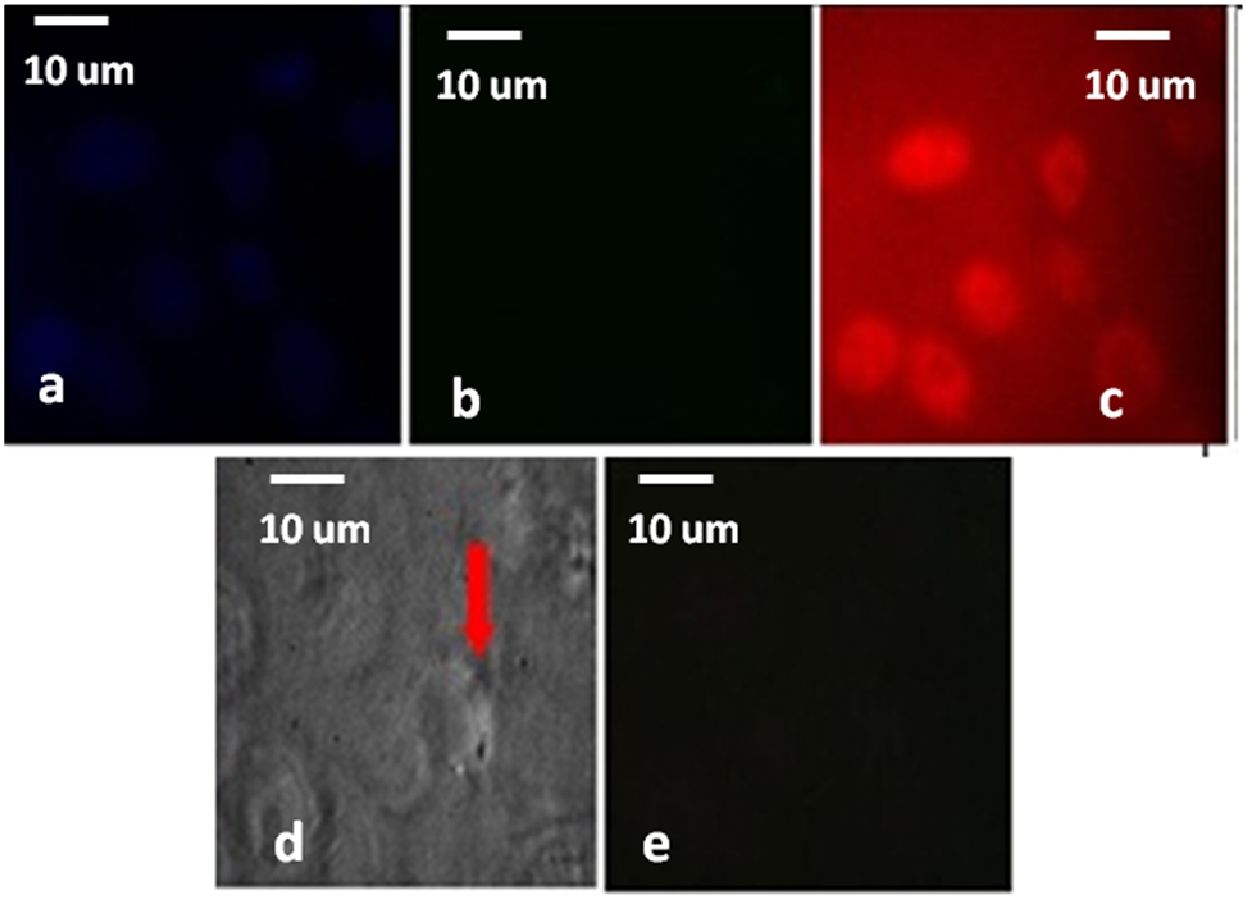

Figure 3-7 Results for MLL-1 (Green) & CTD (Red)

3.3.5 Experiment Set 5

Table 3-5 Experimental Parameters: Set 5

λ = 800nm	Power = ~80mW
t_{ex} = 20 msec	t_{del} = 10 msec
t_{exp} = 10 min	t_{fix} = 7 min

In this set of experiments, the Cytochrome C antibody (Mouse) is available in the green channel and hence the MLL-1 antibody (Rabbit) in the red channel is used so as to be able to distinguish between the two. Post laser irradiation images show evidence of laser damage lines but negligible amount of accumulation in MLL-1 channel and no accumulation in the CytC channel was seen. In Figure 3-8 (a) shows nucleus of HeLa cells stained with DAPI (nuclear stain), (b) CytC staining, (c) MLL-1 staining of the same cells, (d) Post Irradiation image of the same area and (e) Composite Image formed by superimposing images a, b & c

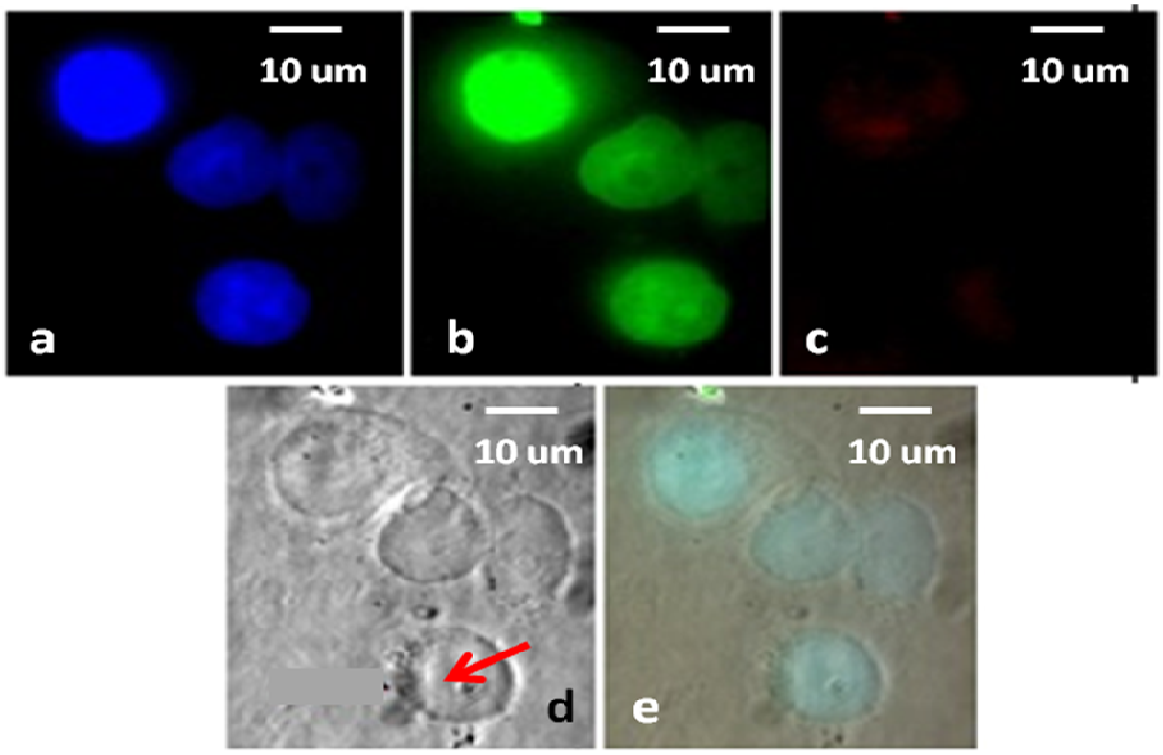

Figure 3-8 Results for CytC (Green) & MLL-1(Red)

3.3.6 Experiment Set 6

Table 3-6 Experimental Parameters: Set 6

λ = 800nm	Power = ~80mW
t_{ex} = 20 msec	t_{del} = 10 msec
t_{exp} = 10 min	t_{fix} = 5 min

In this experiment set, we used MLL-1 (Mouse Antibody) visible in green channel and RBBP5 antibody (Bethyl Lab) visible in the red channel. Each trial shows some positive staining in the RBBP5 channel and 2 out of 3 trails in MLL-1 show positive staining. But these 2 trails also show evidence of laser induced DNA damage (Oxidative stress). In Figure 3-9 (a) shows nucleus of HeLa cells stained with DAPI (nuclear stain), (b) MLL-1 staining of the same cells, (c) RBBP staining, (d) Post Irradiation image of the same area and (e) Composite Image formed by superimposing images a, b & c

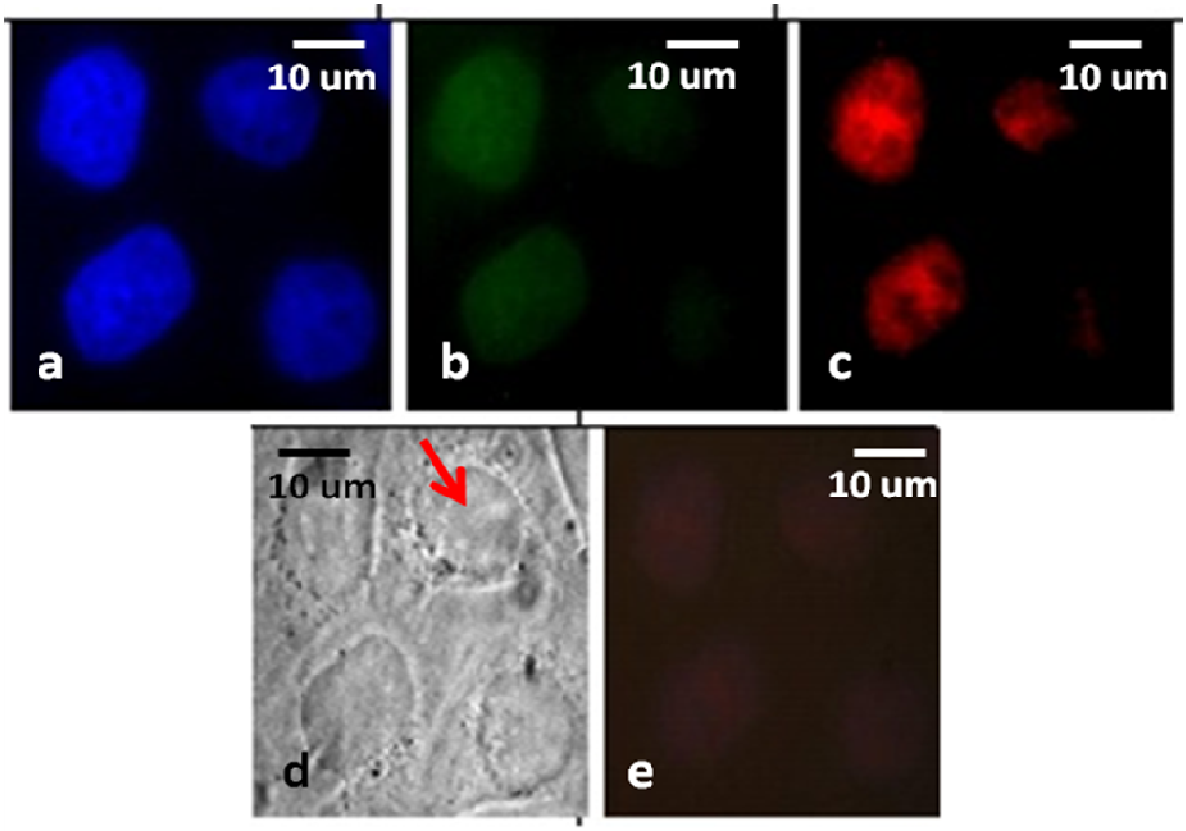

Figure 3-9 Results for MLL-1 (Green) & RBBP (Red)

3.3.7 Irradiation Power constant, t^{fix} varied:

In the next 3 sets of experiment, we have used only 1 antibody (MLL-1). Also we have used DAPI as a nuclear stain to evaluate the co-localization of any positive staining in the MLL channel with the nucleus. Also the fixing time has been varied significantly for these trials while irradiation power is kept constant.

3.3.7.1 Experiment Set: 7, 8, 9

Table 3-7 Experimental Parameters: Set 7, 8, 9

λ = 800nm	Power = ~80mW
t_{ex} = 20 msec	t_{del} = 10 msec

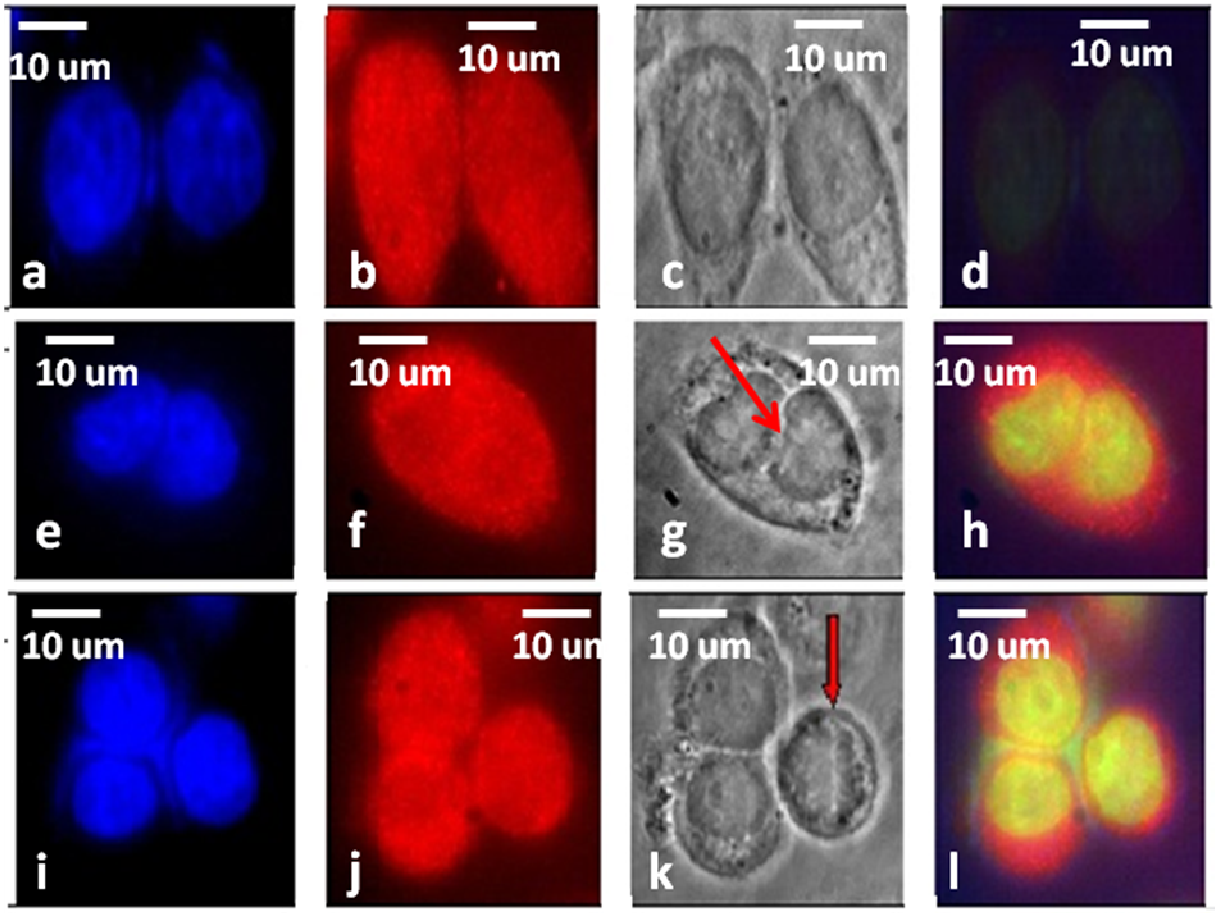

Figure 3-10 Results for MLL-1 with varied fixing times

In Figure 3-10 images (a,e,j) depict nuclei stained with DAPI, (b,f,j) show the staining for MLL-1, images (c,g,k) show the post irradiation images and (d,h,l) are the composite images

formed by super-imposing the MLL and post irradiation channels. The trail shown in row1 had a fixing time of 14 mins, row2 was 7 mins and row3 was 3 mins.

3.3.8 Experiment Set 10 : MLL3

Table 3-8 Experimental Parameters: Set 10

λ = 800nm	Power = ~80mW
t_{ex} = 20 msec	t_{del} = 10 msec
t_{exp} = 10 min	t_{fix} = 10 min

In this set of experiment, the antibody stained for is MLL-3 in the Red channel. It shows some interesting results with the MLL-3 staining being more prominent in certain areas of the nucleus. In Figure 3-11 (a,e) shows DAPI staining in the nucleus of HeLa cells, (b,f) depict MLL-3 staining in the same cells (c,g) Post Irradiation images of the same area and (d,h) Composite Image formed by superimposing image a b & c. 50% of the MLL-3 trails (4 out of 8) showed some accumulation in the MLL-3 channel. The accumulation in MLL-3 co-localizes with the damage line visible in the post irradiation images but is not as distinct and in straight lines as PARP was seen.

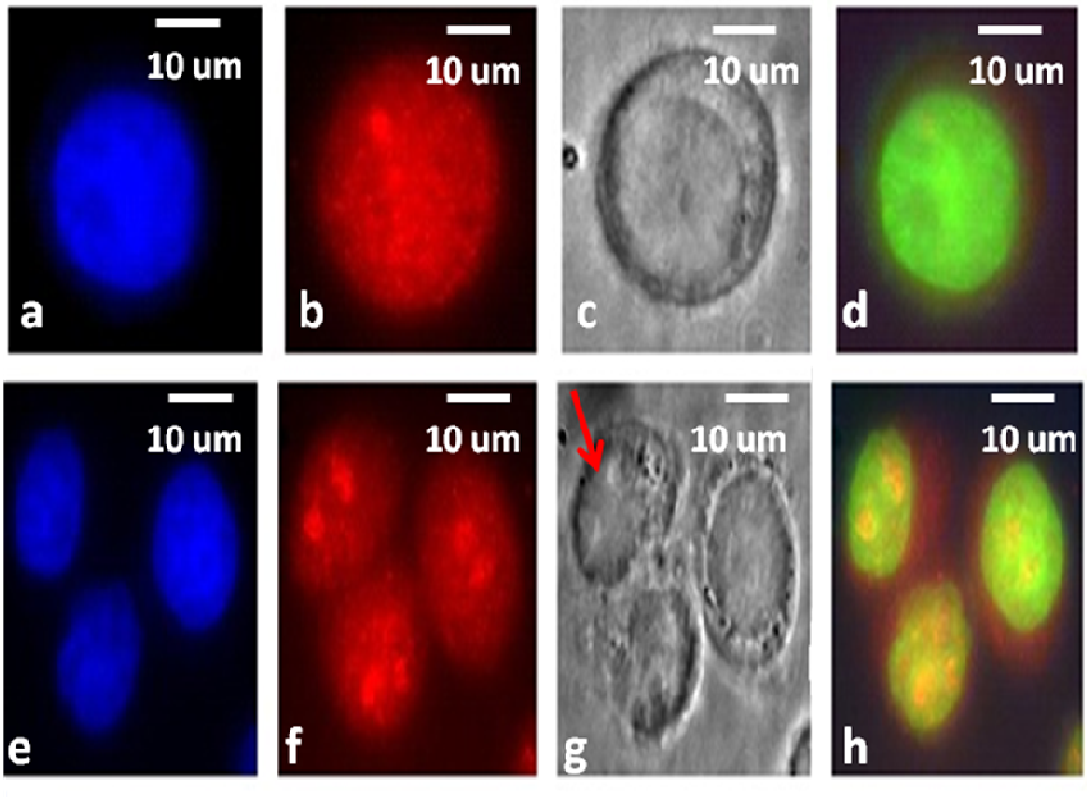

Figure 3-11 Results for MLL-3 [15].

3.3.9 Experiment Set 11, 12: MLL-4

Table 3-9 Experimental Parameters: Set 11

λ = 800nm	Power = ~80mW
t_{ex} = 20 msec	t_{del} = 10 msec
t_{exp} = 10 min	t_{fix} = 3 min

In Figure 3-12 (a,e) DAPI staining, (b,f) MLL-4 (c,g) Post Irradiation and (d,h) Composite Image. DNA damage lines are clearly visible in the post irradiation images but we see no accumulation in MLL-4 staining.

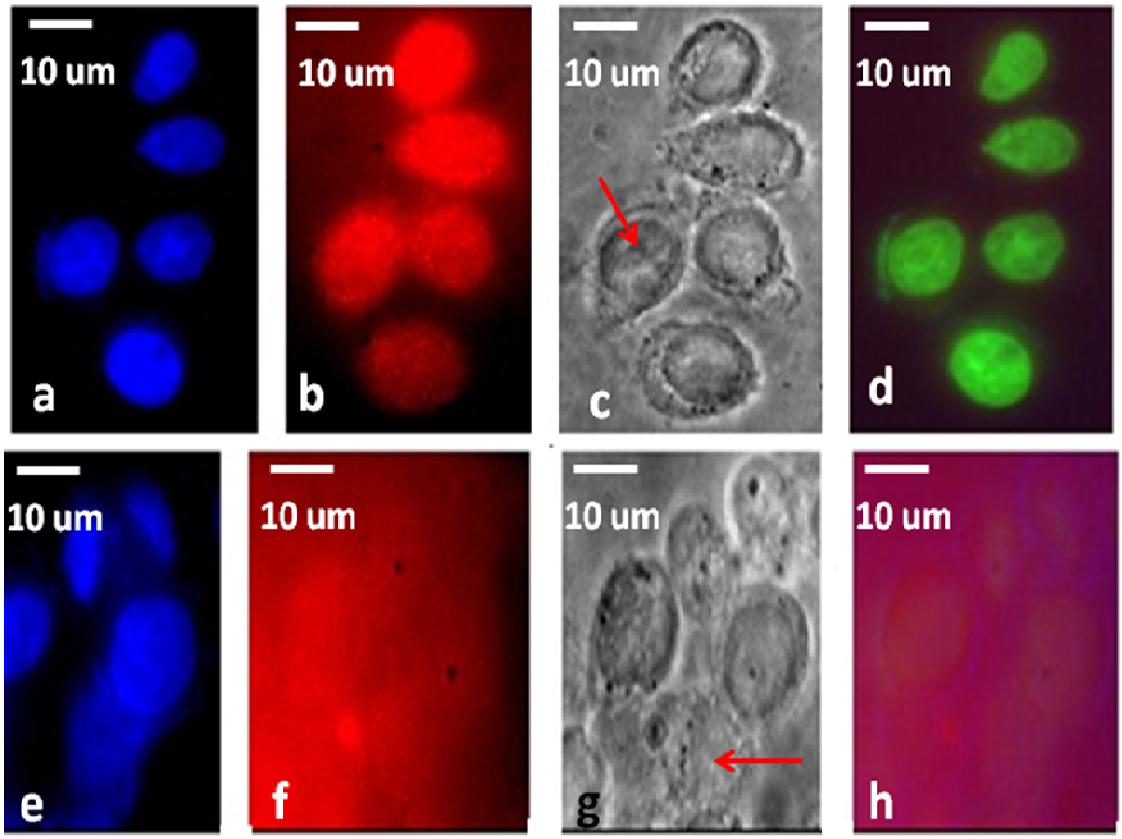

Figure 3-12 Results for MLL-4.

3.4 Discussion

DNA damage lines are clearly with PARP staining with justifies the capability of the system to cause DNA damage. MLL-1 is not seen to co-localize with PARP. When MLL-1 is stained for with CGBP or RBBP5, a few trails show positive staining in the MLL-1 channel. In contrast to it, the bright field (After) channel shows evidence of high levels of DNA damage and MLL-1 accumulation at these sites must be a result of oxidative stress. The trails in which t^{lfix} was varied; it can be hypothesized that the chosen t^{lfix} may not have been sufficient to recruit MLL-1 to the repair sites. MLL-3 is in the same category of MLL proteins as MLL-1 and infact is attached to MLL-1 by another protein sub-unit. Thus it can be thought that MLL-3 might co-

localize with MLL-1 at DNA damage repair sites. In our set of experiments 50% trails for MLL-3 show positive staining in the MLL-3 channel. We could hypothesize the involvement of MLL-3 sub unit prior to MLL-1 in DNA damage repair. More trails on MLL-3 need to be done for rigorous results. MLL-4 does not show any positive staining. Thus the involvement of MLL-1 and its various sub-units and other MLL's was not observed during the course of this study. In order to keep the cell viable before fixing with PFA, the t_{fix} time was varied for different experimental setup. Better knowledge of interactions of proteins with MLL could have given us a better idea of the amount of time taken to for MLL to accumulate to DNA damage site. Depending on this we could have varied the fixing times. With low fixing time, it is possible that the cells are fixed before it has even started to recruit MLL for DNA damage repair.

Chapter 4

Live Cell Method

4.1 TRF2-YFP

A telomere is a region of repetitive nucleotide sequences at each end of a chromosome, which protects the end of the chromosome from deterioration or from fusion with neighboring chromosomes. Telomere regions deter the degradation of genes near the ends of chromosomes by allowing chromosome ends to shorten, which necessarily occurs during chromosome replication. Over time, due to each cell division, the telomere ends become shorter. A telomere acts as a protective cap on chromosome ends, promotes genomic stability, prevents end to end diffusion and disguises chromosome ends. TRF2 stands for Telomeric Repeat Binding Factor 2 and is involved in DNA protection by recruiting other proteins. Dysfunctional TRF2 activates an ATM-mediated DNA damage response pathway whereas over-expression of TRF2 inhibits the same [46]. Depending on the level of TRF2 expression HR and NHEJ pathways are stimulated or inhibited. The debate on TRF2 being an early response to DNA damage has already begun [20] The way the TRF2 experiment has been designed can be used as a model for further experiments.

4.1.1 Results

4.1.1.1 Case 1: Immunostaining

The TRF2-YFP cells were exposed to a continuous laser beam that caused line damage along the nuclei. When these cells were fixed and stained with TRF2 antibody and γ-H2AX, they showed a positive staining in both the channels. γ-H2AX is a confirmatory marker of DSB DNA damage. Since the cells are fixed for immunostaining, the kinetics and dynamics of TRF2 accumulation cannot be studies using this method [10].

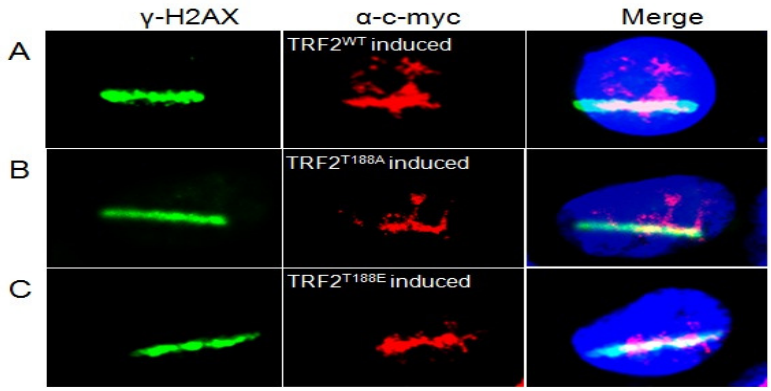

Figure 4-1 Immunostaining of TRF2 along with TUNEL Assay and γ-H2AX.

4.1.1.2 Case 2: Time-lapse epifluorescence of TRF2 accumulation

The image in Figure 4-2 demonstrates the recruitment of TRF2 in a YFP tagged cell over a span of 128 seconds and compares it with a YPF control cell. The 1st laser irradiation is at 4seconds following we observed an increase in fluorescence at that spot. The 2nd pulse was given at 120 seconds to the right of the 1st one and we observed a 2nd fluorescent spot. The control however showed no change in fluorescence.

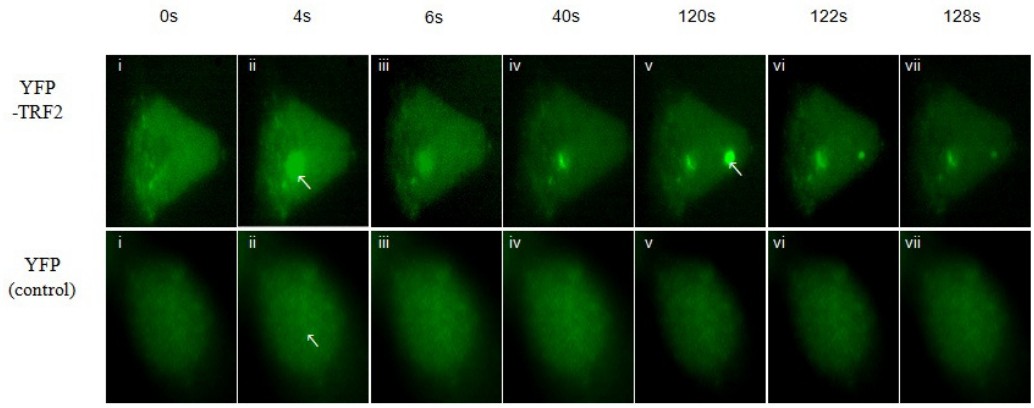

Figure 4-2 Time-lapse imaging of TRF2 accumulation.

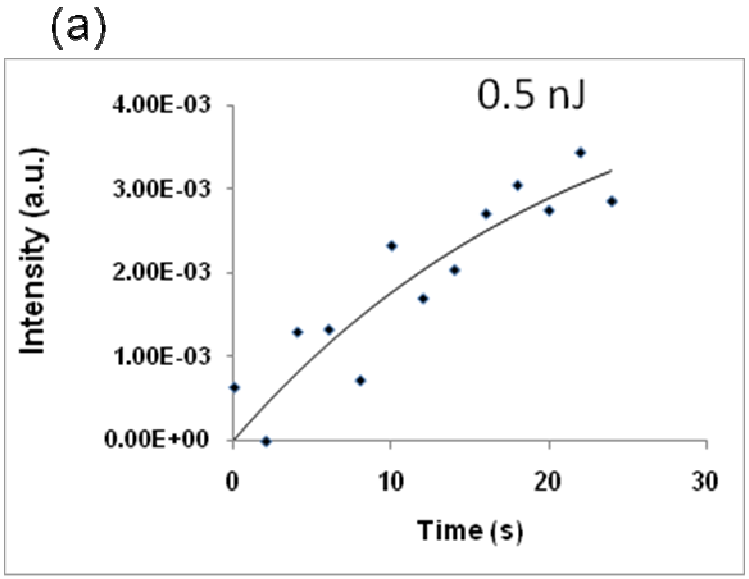

Figure 4-3 Kinetics of increase in fluorescence of TRF2-YFP subsequent to fs laser-induced DNA damage Curve fitting to calculate accumulation time for 0.5nJ pulse

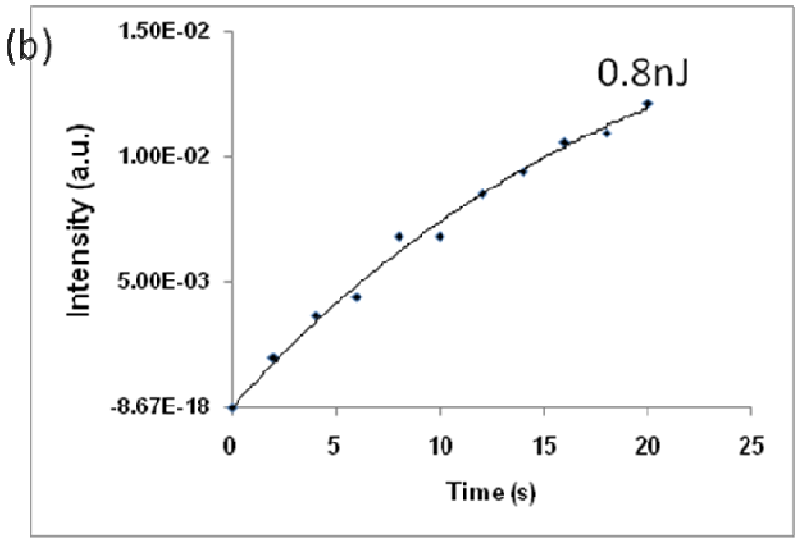

Figure 4-4 Kinetics of increase in fluorescence of TRF2-YFP subsequent to fs laser-induced DNA damage. Curve fitting to calculate accumulation time for 0.8nJ pulse.

The two graphs depict the TRF2 recruitment time fitted to the equation $I=I_0*[1-e^{(-c*t)}]$. The curve on the right is fitted for a 0.5 nJ irradiation and the TRF2 recruitment time is 22.5 sec. The curve on the left is fitted for an irradiation of 0.8nJ and the recruitment time is lesser than the 1st case; ~ 20.5 sec.

From the fluorescence pattern it is observed that a pulse of double the energy induces double the intensity of fluorescence. As already discussed, higher the pulse energy, lower is the accumulation time. Also as the number of pulses is increased, the accumulation time decreases. This is due to the secondary activation of TRF2 proteins at other locations.

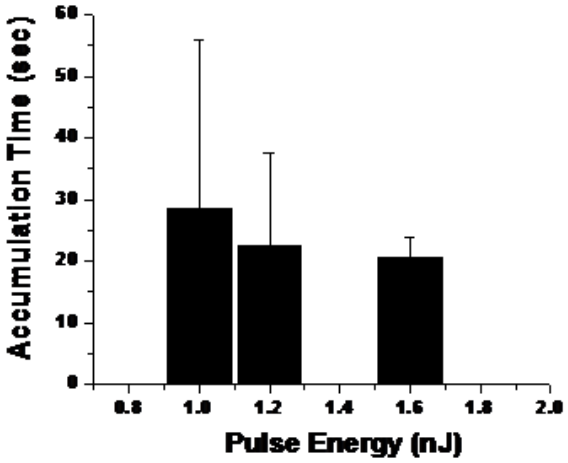

Figure 4-5 Graph of TRF2 Accumulation time v/s Pulse Energy.

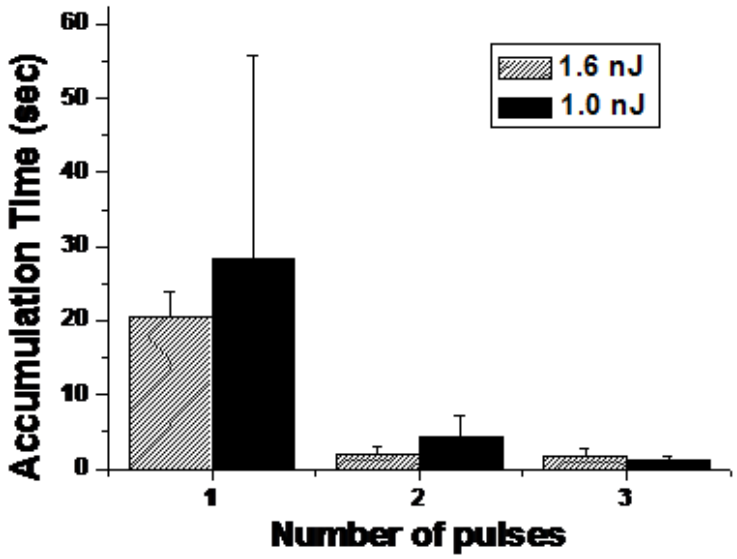

Figure 4-6 TRF2 accumulation time v/s Number of pulses of varying energy.

4.1.2 Discussion

Immunofluorescence shows evidence of TRF2 involvement in DNA damage repair as it co-localizes with γ-H2AX and TUNEL Assay which are marker proteins for DSB DNA damage repair. Time-lapse life time imaging of live cells demonstrated a rise in fluorescence at the spot irradiated by the laser. The increase in fluorescence intensity of the spot is laser wavelength dependant as it depends on the laser power. More laser power leads to higher intensity of fluorescence; also does multiple laser pulses [37].

4.2 HOXB9- GFP (Over-expressed)

Homeobox protein Hox-B9 is a protein that in humans is encoded by the HOXB9 gene [31]. The HOXB9 gene is a member of the Abd-B homeobox family and is included in a cluster of homeobox B genes located on chromosome 17. The encoded nuclear protein functions as a sequence-specific transcription factor that is involved in cell proliferation and differentiation. Studies have shown that HOXB9 is responsive to estrogen and interacts with MLL-1 and MLL-3 via these estrogen-binding sites [15]. Increased expression of this gene is associated with certain

cancers. Homeobox 9 (HOXB9), a non-transforming transcription factor over-expressed in breast cancer, alters tumor cell fate and promotes tumor progression and metastasis [16]. Upon ionizing radiation, ATM is hyper-activated in HOXB9-expressing cells during the early stages of the double stranded DNA break (DSB) response, accelerating accumulation of phosphorylated histone 2AX, mediator of DNA-damage checkpoint 1, and p53 binding protein 1, at DSBs and enhances DSB repair.

4.2.1 Results

A total number of 6 trials were performed to investigate the recruitment of HOXB9-GFP to the DNA damage site upon spot irradiation by a laser beam. In all the trials, multiple laser pulses were given to the cell. The parameters used for the 6 trials are given in Table 4-1 All the trails ran for 300 seconds with the acquisition rate being 1 frame/ sec. While running the trails, there was no visible change in the fluorescence of the cells which compelled us to administer extra laser pulses to see the effect.

Table 4-1 Experimental Parameters for HoxB9

λ = 800 nm
t_{exp} = 20msec – 40 msec
Power = ~80mW

Once the time-lapse images are acquired, they are processed to investigate a change in fluorescence at the spot at which the laser beam irradiates the cell. Using ImageJ, a 30x30 small square area is cropped at the laser spot and the integrated intensity over that area for all 300 frames was calculated. The same was done for a 30x30 are elsewhere in the same fluorescent cell. The integrated intensity of the spot area was divided by that of the control area to obtain a normalized form. The data from only 2 trails are shown below.

4.2.1.1 Trail 1

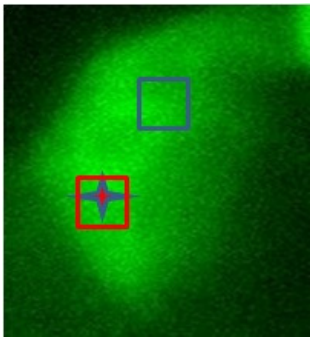

Figure 4-7 HoxB9-GFP (Trail 1).

The above image shows a fluorescent HEK-HOXB9-GFP cell. The blue star signifies the laser spot and the red box is the spot area and the blue box is the control area. A total of 8 pulses were used in this trial. As it can be seen from the Intensity v/s Time plot shown in Figure 4-8, the initial pulses (λ = 785nm) are not evident in the plot. After the wavelength was increased, the pulses at frame 178, 260 are visible. The intensity peaks correspond to the sudden burst of energy due to the laser spot. After the laser exposure, the fluorescence returned to the baseline without any significant change. In the normalized plot the increase in fluorescence after the 2nd peak is not significant.

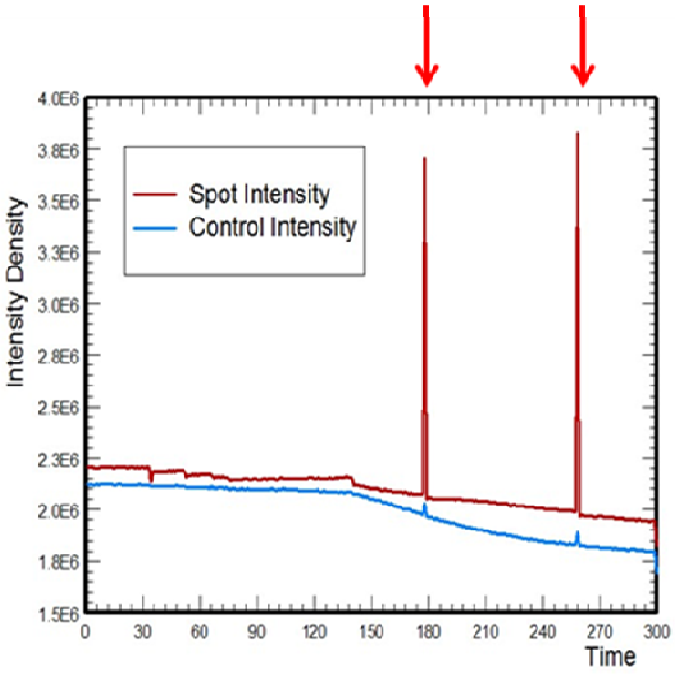

Figure 4-8 Intensity v/s Time plot.

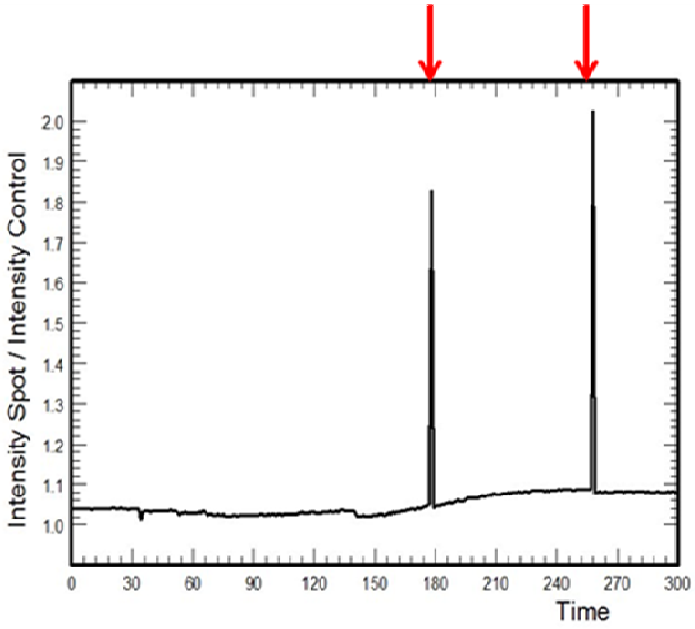

Figure 4-9 Normalized Plot.

4.2.1.2 Trial 2

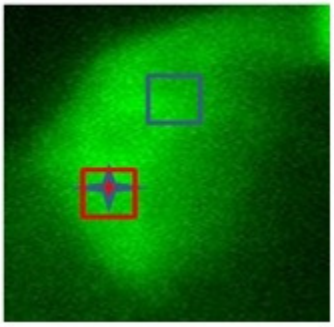

Figure 4-10 HoxB9-GFP (Trial 2).

The data was processed in the same way as trial 1. The total number of pulses in this trial are 5 out of which 2 (Frame 75 and 121) are clearly visible. As seen from the Intensity v/s Time plot, the base fluorescence in the control region was higher than that in the spot until after the 1st laser pulse. A few seconds after the 1st laser pulse the fluorescence in both the regions changed significantly. But after the 2nd significant laser pulse, there is no significant increase in fluorescence as it can be seen from the normalized plot.

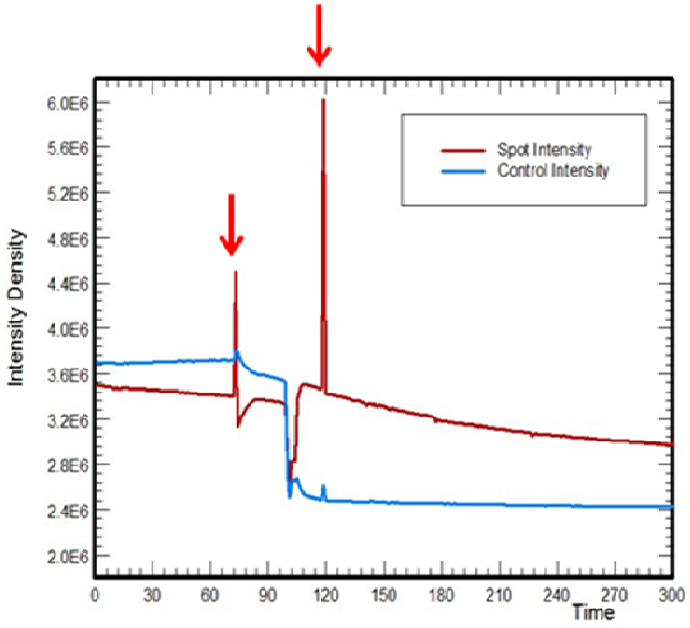

Figure 4-11 Intensity v/s Time plot.

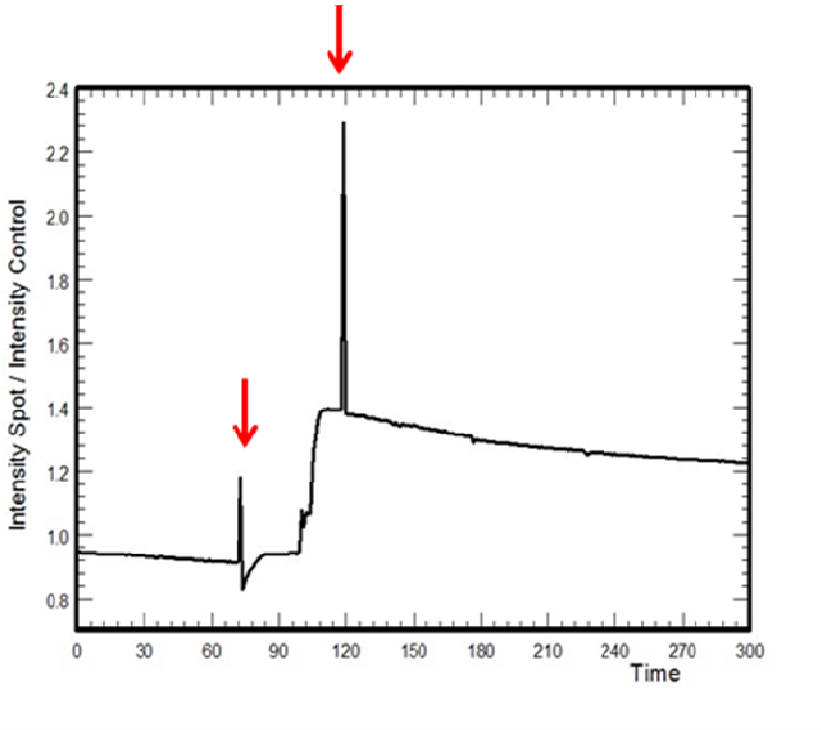

Figure 4-12 Normalized Plot.

4.2.2 Discussion

It is already known that HoxB9 is over-expressed in breast cancer conditions. Also HoxB9 induces radiation resistance in HoxB9-expressing-MCF10A cells and increases the survival of these cells post exposure to radiation. It is also observed that the number of foci exhibiting γ-H2AX (A DNA DSB marker) and 53BP foci is higher in HoxB9 over-expressing cells. A different study has shown that, higher the level of HoxB9 expression, higher is the tumor grade [17]. Also HoxB9 induces the expression of other factors which activate their respective pathways to increase tumor activity. Since just 1 out of 6 trials of HoxB9 recruitment to DNA damage site showed significant increase in fluorescence, it can be hypothesized that HoxB9 is not directly involved in DNA damage repair. But is involved by recruiting other proteins and the expression of these proteins are regulated by the level of Hoxb9 expression.

Chapter 5

Conclusion & Future Work

In our course of experiment, we have tried to closely analyze the interaction of repair protein with one another and in the bigger picture tried to study their role in DNA damage response/ repair pathway. MLL-1 and its sub units like CGBP and RBBP5 we studied with respect to PARP, a formerly known repair protein, involved in DNA damage repair. Some sub-units could not be stained with PARP because of incompatibility of anti-body and some were in the same excitation-emission channel as PARP. Other MLL trials did not reveal much about MLL's role in DNA damage repair pathway. 50% of MLL 3 trails showed presence of MLL-3 accumulation but were not co-localized with the bright-field images. MLL 4 did not show any signs of protein accumulation. This can be termed as the Direct or Fixed method of analyzing cells the cells are fixed post laser irradiation and screened for antibodies by immunostaining. We can at most screen for 2 proteins at a time depending on their anti-body compatibility. As the cells are fixed post irradiation, the fixation time (t_{fix}) is crucial in these experiments. All repair proteins have their own respective response times which is the time taken for them to accumulate at the DNA damage site. The fixation times in these experiments were not more than 15 mins which was a constraint, in order to maintain the viability of cells. A short fixation time may not be sufficient enough for MLL or any of its sub-units to accumulate at the DNA damage sites. A better understanding of the interaction of MLL and other known repair proteins of the various pathways will make it clear if MLL is involved in the DNA damage recognition/ repair process.

Experiments with TRF2, to study its accumulation at DNA damage sites and to verify if TRF2 can be thought to be as an early responder to DNA damage, broadens the scope of research to study the behavior of other similar proteins. The results of these experiments give us a clear idea of TRF2 being a part of the early response mechanism (Response time is in seconds). Also the quantity of TRF2 accumulation is non-linear and wavelength dependant. It

also depends on the laser pulse power and the number of pulses applied. We further use the TRF2 experimental model to screen if HoxB9 is involved in the process of DNA damage recognition/ repair. We have some interesting results in the Live cell Method. 5 out of 6 trials of HoxB9 were negative in terms of increase in fluorescence post laser- irradiation. But according to the work done by other research groups, increased HoxB9 activity is observed in certain cancers and the cellular response to such conditions is by activating other related proteins and enzymes. It is likely that these other proteins might play an active role in the DNA damage repair pathway indirectly via HoxB9.

Future work can be extended from the current study to further new proteins and cell lines. In order to verify if MLL is involved in the process of DNA damage recognition/ repair or not we can check for the co-localization of MLL with other known repair proteins like Ku70, DNA-Pkcs and YH2AX. If MLL co-localizes with any of these, it gives a better understanding of the pathway by which MLL is activated and thus renders a new direction to this study. It is proposed to study the response of cells in which MLL is knocked down using anti-sense. If the response to DNA damage in these cells is inhibited, MLL is likely to be involved in the process of DNA damage recognition/ repair. The TRF2 model can be extended to MLL by tagging the MLL protein with M-Cherry. Lifetime imaging of MLL can be made possible which allows us to study its interaction in real-time.

To comprehensively understand the role of HoxB9 in DNA damage recognition/ repair we can extend the current study to a comparative study of HoxB9 overexpressed cells v/s control cells (Normal HoxB9 distribution) v/s HoxB9 - ΔD (Homeodomain deleted). This will make it clear if HoxB9 is directly involved in DNA damage repair or has an indirect role by recruiting other repair proteins. Screening of Hoxb9 can be used to formulate a model based on which other Hox proteins can be screened. We can study the interactions of TRF2, MLL and Hox proteins by studying TRF2 recruitment to DNA damage sites in MLL knockdown cells and HoxB9 over expressing cells. This can lead to some novel discovery about the functioning of

these repair proteins. Finally the TRF2 kinetics data which proves TRF2 accumulation at DNA damage sites can be analyzed using a confocal setup with Raster Image Correlation Spectroscopy (RICS) technique in order to study the dynamics of TRF2 accumulation.

Appendix A

List of Abbreviations

DNA	Deoxyribonucleic Acid
RNA	Ribonucleic Acid
MLL	Mixed Lineage Leukemia
HOXB9	Homeobox Protein B9

Appendix B

Presentation in Conferences

1. ‘Role of MLL in DNA Damage repair’ (Poster) Annual Celebration of Excellence by Students Symposium, UTA, Arlington, Tx (March 2012)
2. ‘Diffusion Dynamics of Trf2 Recruitment in Cells towards DNA Damage-Sites Caused by Ultrafast Near-Ir Laser Micro-Irradiation’ (Oral Presentation) SPIE Optics & Photonics 2012, San Diego, CA (August 2012)

References

1. Gong, Z., Cho, Y. W., Kim, J. E., Ge, K., and Chen, J. “Accumulation of Pax2 transactivation domain interaction protein (PTIP) at sites of DNA breaks via RNF8-dependent pathway is required for cell survival after DNA damage”,2009, J Biol Chem 284, 7284-7293.
2. Dinant, C., de Jager, M., Essers, J., van Cappellen, W. A., Kanaar, R., Houtsmuller, A. B., and Vermeulen, W. “Activation of multiple DNA repair pathways by sub-nuclear damage induction methods”, 2007, J. Cell Sci. 120, 2731-2740
3. S.H. Kaufmann, G. Brunet, B. Talbot, D. Lamarr, C. Dumas, J.H. Shafer, G. Poirier “Association of poly(ADP–ribose) polymerase with the nuclear matrix: the role of intermolecular disulfide bond formation, RNA retention and cell type” Exp. Cell. Res, 1991, 524-535
4. Shiloh, Y “ATM and related protein kinases: safeguarding genome integrity”, 2003, Nat Rev Cancer 3, 155-168
5. Taylor, A. M. R. “Chromosome instability syndromes”, 2001, Best Pract, Res. Clin. Haematol. 14, 631-644
6. Kui Shin Voo, Diana L. Carlone, Britta M. Jacobsen, Anna Flodin, and David G. Skalnik* “Cloning of a Mammalian Transcriptional Activator That Binds Unmethylated CpG Motifs and Shares a CXXC Domain with DNA Methyltransferase, Human Trithorax, and Methyl-CpG Binding Domain Protein 1”, Molecular and cell Biology, 2000, March
7. S. K. Mohanty, A. Rapp, S. Monajembashi, P. K. Gupta and K. O. Greulich “Comet Assay Measurements of DNA Damage in Cells by Laser Microbeams and Trapping Beams with Wavelengths Spanning a Range of 308 nm to 1064 nm”, Rad. Research

8. Xiangduo Kong, Samarendra K. Mohanty, Jared Stephens, Jason T. Heale, “Comparative analysis of different laser systems to study cellular responses to DNA damage in mammalian cells”, Nucleic Acid Res., 2009
9. Munoz, I. M., and Rouse, J. “Control of histone methylation and genome stability by PTIP”, 2009, EMBO Rep 10, 239-245
10. Huda, N., Tanaka.H, Mendonca .M. S, and Gilley. D, “Damage-induced phosphorylation of TRF2 is required for the rapid stage of DNA double-strand break repair”, 2009, Molecular & Cellular Biology, 3597–3604.
11. Ninad Ingle “Development of Multimodal imaging system combined with laser microbeam for nano-scale manipulation and characterization”, Thesis, UTA May 2011
12. Verger, A., and Crossley, M. “DNA damage repair and transcription: Chromatin modifiers in transcription and DNA repair”, 2004, Cellular and Molecular Life Sciences CMLS 61, 2154-2162.
13. S Dambacher1, 2, M Hahn1,2 and G Schotta1 “Epigenetic regulation of development by histone lysine methylation”, Heredity, 2010
14. Matthew G. Guenther*, Richard G. Jenner*, Brett Chevalier*, Tatsuya Nakamura Carlo M. Croce Eli Canaani & Richard A. Young “Global and Hox-specific roles for the MLL1 methyltransferase”, 2005, PNAS
15. Ansari, K. I., Shrestha, B., Hussain, I., Kasiri, S., and Mandal, S. S. “Histone Methylases MLL1 and MLL3 Coordinate with Estrogen Receptors in Estrogen-Mediated HOXB9 Expression”, Biochemistry 50, 3517-3527
16. Naokazu Chibaa, b, Valentine Comaillsc, Bunsyo Shiotanib, Fumiyuki Takahashia,b, Toshiyuki Shimadaa,b, Ken Tajimaa,b, “Homeobox B9 induces epithelial-to-

mesenchymal transition-associated radioresistance by accelerating DNA damage responses", PNAS 2011

17. Hayashida, Tetsu "HOXB9, a gene overexpressed in breast cancer,promotes tumorigenicity and lung metastasis" PNAS 2009
18. Khairul I. Ansari1, Bibhu P. Mishra1, Subhrangsu S. Mandal "Human CpG binding protein interacts with MLL1, MLL2 and hSet1 and regulates Hox gene expression", Biochimica et Biophysica Acta (BBA) - Gene Regulatory Mechanisms, 2008
19. Jowsey, P. A., Doherty, A. J., and Rouse, J. "Human PTIP facilitates ATM-mediated activation of p53 and promotes cellular resistance to ionizing radiation", 2004, J Biol Chem 279, 55562-55569.
20. Paul S Bradshaw, Dimitrios J Stavropoulos and M Stephen Meyn "Human telomeric protein TRF2 associates with genomic double-strand breaks as an early response to DNA damage", Nature Genetics, 2005
21. Fernandez-Capetillo, O., Lee, A., Nussenzweig, M., and Nussenzweig, A. "H2AX: the histone guardian of the genome", 2004, DNA Repair 3, 959-967
22. S Ziemin-van der Poel, N R McCabe, H J Gill, R Espinosa, III, Y Patel, A Harden, P Rubinelli, S D Smith, M M LeBeau, J D Rowley "Identification of a gene, MLL, that spans the breakpoint in 11q23 translocations associated with human leukemias.", PNAS, 1991, December
23. Josée Guirouilh-Barbat, Sylvie Huck, Pascale Bertrand, Livia Pirzio, Chantal Desmaze, Laure Sabatier, Bernard S. Lopez "Impact of the KU80 Pathway on NHEJ-Induced Genome Rearrangements in Mammalian Cells" Molecular Cell 2004
24. Yokoyama, A., Wang, Z., Wysocka, J., Sanyal, M., Aufiero, D. J., Kitabayashi, I., Herr, W., and Cleary, M. L. "Leukemia proto-oncoprotein MLL forms a SET1-like

histone methyltransferase complex with menin to regulate Hox gene expression", 2004, Mol Cell Biol 24, 5639-5649.

25. Ansari, K. I., Kasiri, S., Hussain, I., and Mandal, S. S. "Mixed lineage leukemia histone methylases play critical roles in estrogen-mediated regulation of HOXC13", 2009, FEBS J 276, 7400-7411.
26. Ansari, K. I., and Mandal, S. S. "Mixed lineage leukemia: roles in gene expression, hormone signaling and mRNA processing", 2010, FEBS J 277, 1790-1804.
27. Ansari, K. I., Mishra, B. P., and Mandal, S. S, "MLL histone methylases in gene expression, hormone signaling and cell cycle", 2009, Front Biosci 14, 3483-3495.
28. Armstrong, S. A., Staunton, J. E., Silverman, L. B., Pieters, R., den Boer, M. L., Minden, M. D., Sallan, S. E., Lander, E. S., Golub, T. R., and Korsmeyer, S. J. "MLL translocations specify a distinct gene expression profile that distinguishes a unique leukemia", 2002, Nat Genet 30, 41-47.
29. Melissa M Steward, Jung-Shin Lee, Aisling O'Donovan, Matt Wyatt, Bradley E Bernstein & Ali Shilatifard "Molecular regulation of H3K4 trimethylation of ASH2L, a shared sub-unit of MLL complexes", Nature Structural & Molecular Biology, 2006
30. Lukas, J., Lukas, C., and Bartek, J. "More than just a focus: The chromatin response to DNA damage and its role in genome integrity maintenance", 2011, Nat Cell Biol 13, 1161-1169
31. Phyllis J. McAlpine∗, Thomas B. Shows "Nomenclature for human homeobox genes", Genomics, 1990
32. Camille Godon, Fabrice P. Cordelières, Denis Biard, Nicole Giocanti, Frédérique Mégnin-Chanet, Janet Hall & Vincent Favaudon "PARP inhibition versus PARP-1 silencing: different outcomes in terms of single-strand break repair and radiation susceptibility" Nucleic Acids Res., 2008 August

33. Nucleic Acids Res. “Poly(ADP-ribose) polymerase (PARP-1) has a controlling role in homologous recombination” Nucleic Acids Res, 2003 September
34. F. Javier Oliver, Josiane Menissier-de Murcia, and Gilbert de Murcia “Poly (ADP-Ribose) Polymerase in the Cellular Response to DNA Damage, Apoptosis, and Disease” Am. J. Hum. Genet, 1999, 64: 1282-1288
35. Mark R. Cooksona, ,Paul G. Inceb, Philip A. Ushera, Pamela J. Shawa, “Poly(ADP–ribose) polymerase is found in both the nucleus and cytoplasm of human CNS neurons”
36. Young-Wook Cho, Teresa Hong, SunHwa Hong, Hong Guo, Hong Yu, Doyeob Kim, Tad Guszczynski, Gregory R. Dressler, Terry D. Copeland, Markus Kalkum & Kai Ge, “PTIP Associates with MLL3- and MLL4-containing Histone H3 Lysine 4 Methyltransferase Complex”, 2007, The Journal of Biological Chemistry, 282,20395-20406
37. Nazmul Huda, Satoshi Abe, Gu Ling, Marc S. Mendonca, Samarendra Mohanty & David Gilley “Recruitment of TRF2 to laser-induced DNA damage sites”
38. Yali Dou, Thomas A Milne, Alexander J Ruthenburg, Seunghee Lee, Jae Woon Lee, Gregory L Verdine C David Allis2 & Robert G Roeder1 “Regulation of H3K4 methyltransferase activity by its core components”, Nature Structural & Molecular Biology, 2006
39. M.S. Satoh, T. Lindahl ,“Role of poly(ADP–Ribose) formation in DNA repair” Nature 1992, 356-358
40. Waldman, A S Waldman & B C “Stimulation of intrachromosomal homologous recombination in mammalian cells by an inhibitor of poly (ADP-ribosylation).” Nucleic Acids Res, 1991, November

41. Vanja Avdic, 1,3 Pamela Zhang,1,3 Sylvain Lanouette,1 Adam Groulx,1 Ve´ ronique Tremblay,1 Joseph Brunzelle,2 “Structural and Biochemical Insights into MLL1 Core Complex Assembly”, Cell Press
42. D. Lamarre, B. Talbot, G. deMurcia, C. Laplante, Y. Leduc, A. Mazen, G.G. Poirier “Structural and functional analysis of poly(ADP ribose) polymerase: an immunological study” Biochem. Biophys. Acta, 1988, 147-160
43. G. DeMurcia, V. Schreiber, M. Molinete, B. Saulier, O. Poch, M. Masson, C. Niedergang, J. MénissierDeMurcia “Structure and function of poly(ADP–ribose) polymerase”
44. Huen, M. S. Y., and Chen, J. “The DNA damage response pathways: at the crossroad of protein modifications” 2008, Cell Res 18, 8-16
45. Juliane Lüscher-Firzlaff et al. “The Human Trithorax Protein hASH2 Functions as an Oncoprotein”, 2008, Cancer Res.
46. Jan Karlseder, Kristina Hoke, Olga K. Mirzoeva, Christopher Bakkenist, Michael B. Kastan, John H. J. Petrini, Titia de Lange “The Telomeric Protein TRF2 Binds the ATM Kinase and Can Inhibit the ATM-Dependent DNA Damage Response”, 2004, PLOS Biology
47. Joanna Wysocka, Tomek Swigut, Thomas A. Milne, Yali Dou, Xin Zhang, Alma L. Burlingame, Robert G. Roeder, Ali H. Brivanlou and C. David Allis “WDR5 Associates with Histone H3 Methylated at K4 and Is Essential for H3 K4 Methylation and Vertebrate Development”, Cell 2005
48. www.atlasgeneticsoncology.org
49. www.cellbiolabs.com
50. www.nextprot.org

Biographical Information

Somdutta Chakraborty has her undergraduate degree, Bachelor's in Biomedical Engineering from the University of Mumbai, India. She has worked at Dr.L.H Hiranandani Hospital, Mumbai, India as a Biomedical Engineer Intern in 2009 (July-Dec) She worked as a part of a team on a Matlab based project for Iris Recognition, under the guidance of Prof. Dhananjay Theckedath, as a part of her senior year project. She was admitted to The University of Texas at Arlington for her Master of Science degree in Bioengineering. She joined the Biophysics & Physiology group in July 2011 as a step towards completing her thesis. She worked with Dr. Samarendra Mohanty in the Physics Department on 'Involvement of Mixed Lineage Leukemia and Homeobox Proteins in DNA Damage Recognition and Repair' for her M.S thesis research. She graduated from UTA in Fall 2012. Her areas of academic interest are Medical Imaging, Digital Image Processing and Cancer-based research.